# PERFECT MATCHINGS AND APPLICATIONS

Mihai Ciucu

Department of Mathematics, Indiana University, Bloomington, IN 47405

*To David and Ane*

# Contents

# Preface

These lectures were given in a graduate course while I visited Kyushu University between April and July 2009. Of invaluable help to me as I wrote up these lectures were the wonderfully detailed class notes taken by Shingo Saito. It was a pleasure to teach this course. I would like to thank Professor Masato Wakayama for the invitation to visit Kyushu University and for his generous support. I would also like to thank him and his wife Chieko for their warm hospitality, due to which my wife, our two year old son and I felt in Fukuoka like in a home away from home. Several people contributed to us feeling so welcome, including Professors Kaneko and Gon and their families, and the dean's secretary Nakaoka-san, who answered my many questions with amazing helpfulness and good will. And last but not least, I thank all the people who listened to my lectures, and especially Shingo Saito, whose detailed following and insightful questions were a great help throughout this course.

Mihai Ciucu
January 2010

## Introduction

A *graph* $G = (V, E)$ consists of a set $V$ of vertices together with a collection $E$ of 2-element subsets of $V$ called edges. All graphs considered in this course will have a finite number of vertices.

A *perfect matching* of a graph is a collection of disjoint edges which cover all vertices. For instance, the graph pictured in Figure 1.1(a) has a total of three perfect matchings, indicated in Figure 1.1(b). We denote the number of perfect matchings of a graph $G$ by $\mathrm{M}(G)$.
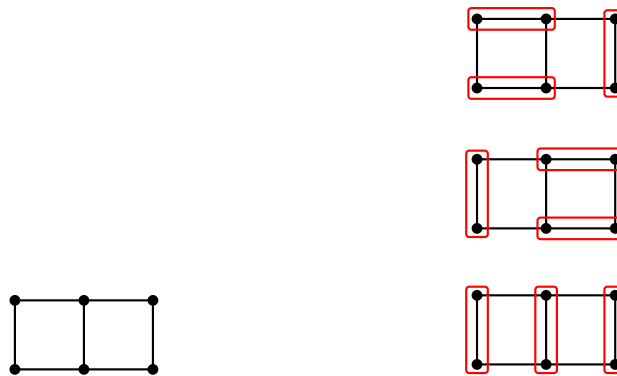


FIGURE 1.1(a). A graph on six vertices. FIGURE 1.1(b). Its three perfect matchings.

Let us look now at a larger example. Suppose we want to find all perfect matchings of the 12-vertex graph shown on the left of Figure 1.2. We branch in two possibilities according to whether the top leftmost vertex is matched horizontally or vertically. In the former case, three other edges (encircled by dotted lines in Figure 1.2) are forced to be part of the perfect matching, and what is left uncovered is just a 4-cycle, which clearly has two perfect matchings. The latter case further branches into two, according as the left topmost vertex is matched horizontally or vertically. Now the vertically matched instance forces 2 edges, leaving two ways to finish this subcase. The horizontally matched alternative branches in two more sub-branches; each of them is readily seen to have exactly two ways of completing them to a perfect matching (see the figure). Thus the total number of perfect matchings of this graph is 8.

A final example we do "by hand" is the $4 \times 4$ grid graph $G_4$, illustrated in Figure 1.3. We branch in two according as the top left vertex is matched horizontally or vertically; by symmetry the two cases can be extended to a perfect matchings in the same number of ways. Figure 1.3 describes the top branch as it further divides into sub-branches, depending on how certain vertices are matched. The number of ways to finish the partial matchings at the tips of the tree is readily found to be as indicated in the picture. We obtain $\mathrm{M}(G_4) = 36$.
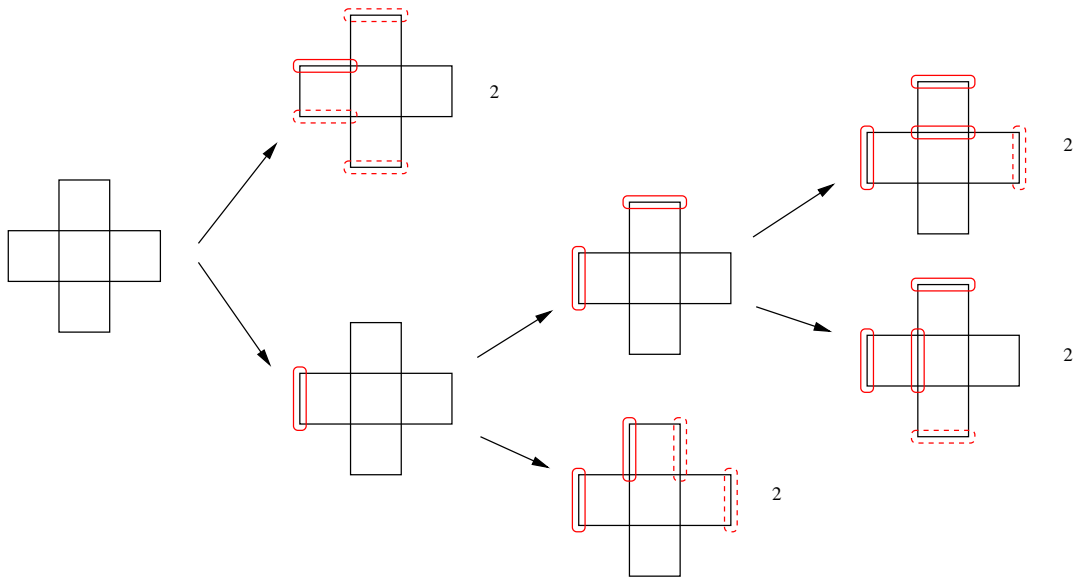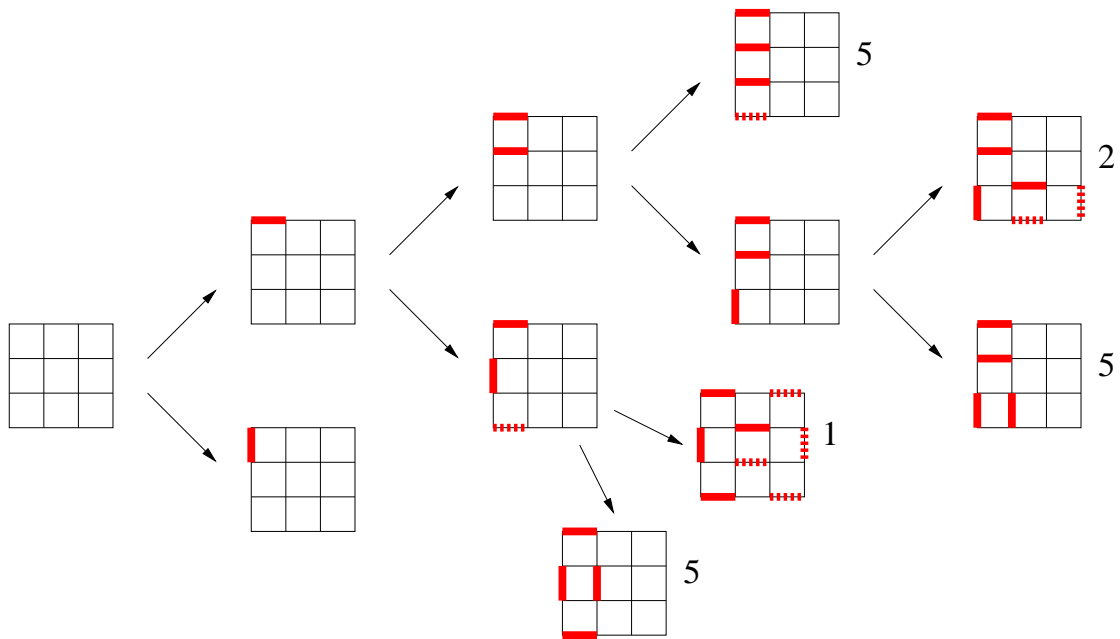
FIGURE 1.2. A larger graph and its eight perfect matchings.



FIGURE 1.3. The 36 perfect matchings of the $4 \times 4$ grid graph $G_4$.

Now here is a useful trick that can be used to get the above answers more quickly. It turns out (this is a special case of Theorem 10.2 that we will prove later in the course) that if you have a subgraph $G$ of $\mathbb{Z}^2$ that is symmetric with respect to a diagonal lattice line $\ell$, then if you scan the vertices of $G$ on $\ell$ from left to right and alternately remove the edges incident to them from above $\ell$ and from below $\ell$, then the resulting subgraph

4

$G'$ is such that

$$\mathrm{M}(G) = 2^k \, \mathrm{M}(G'), \tag{1.1}$$

where $2k$ is the number of vertices of $G$ on $\ell$ (this number is even if $G$ admits perfect matchings, as this requires $G$ to have an even number of vertices in total, and the vertices off $\ell$ come in pairs, due to the symmetry of $G$).

Applying (1.1) to the graph $G_4$ we get



But the graph on the right has two connected components, each isomorphic to the graph in Figure 1 after removal of one forced edge. Thus we recover the answer $2^2 \cdot 3^2 = 36$, which was obtained by "brute force" earlier. A similar application of (1.1) to the graph in Figure 1.2 provides its number of perfect matchings as $2^1 \, \mathrm{M}(C_4)^2 = 8$, as the 4-cycle $C_4$ clearly has two perfect matchings.

Consider now the following sequence of graphs:
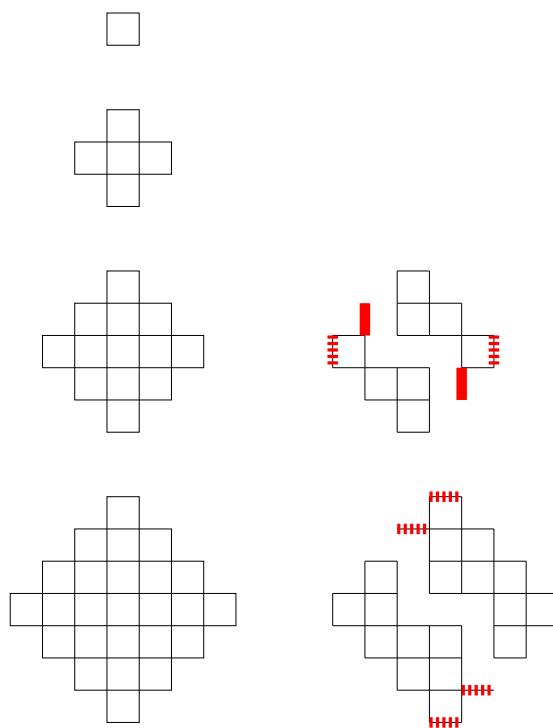


Denoting the $n$-th graph in this sequence by $AD_n$, we clearly have $\mathrm{M}(AD_1) = 2$ and $\mathrm{M}(AD_2) = 8 = 2^3$. By (1.1) and the picture above, a simple perfect matching

count of the resulting small graph gives $M(AD_3) = 2^2 \cdot 4^2 = 2^6$. One similarly obtains $M(AD_4) = 2^2 \cdot 16^2 = 2^{10}$. So it looks like $M(AD_n) = 2^{n(n+1)/2}$ for all $n$. This is indeed the case, as we will show in the next lecture (see Theorem 2.1).

We conclude the introduction by mentioning two classical results in the subject of counting perfect matchings of graphs. The first concerns the $m \times n$ grid graph $G_{m,n}$, of which the special case $m = n = 4$ is illustrated in Figure 1.3. In the mid-1930's, physicists considered the problem of modeling the adsorption of a liquid by the face of a crystal immersed in it. Assuming the crystal face has a square lattice structure and that the liquid has diatomic molecules whose lengths are equal to the lattice spacing, this associates to each "fully packed" adsorption configurations a perfect matching of the grid graph. The solution came 25 years later, when Kasteleyn and independently Temperley and Fisher proved the following result.

THEOREM 1.1. *For any positive integers $m$ and $n$ one has*

$$M(G_{2m,2n}) = 2^{2mn} \prod_{j=1}^{m} \prod_{k=1}^{n} \left( \cos^2 \left( \frac{j\pi}{2m+1} \right) + \cos^2 \left( \frac{k\pi}{2n+1} \right) \right).$$

The final result we mention here concerns a family of graphs on the hexagonal lattice. For any positive integers $a$, $b$ and $c$ let $H_{a,b,c}$ be the "honeycomb graph" obtained by taking an $a \times b \times c \times a \times b \times c$ array of unit hexagons on the regular hexagonal lattice (Figure 1.4 illustrates $H_{4,2,3}$). Around 1900 MacMahon proved a result equivalent to the following.
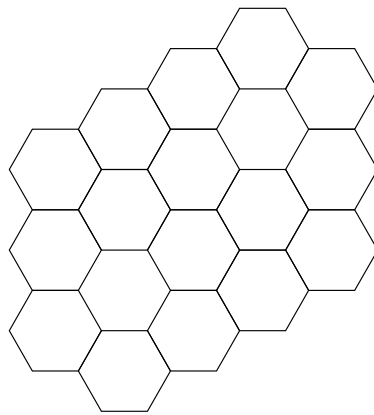


FIGURE 1.4. The $4 \times 2 \times 3$ honeycomb graph $H_{4,2,3}$.

THEOREM 1.2. *For any positive integers $a$, $b$ and $c$ one has*

$$M(H_{a,b,c}) = \prod_{i=1}^{a} \prod_{j=1}^{b} \prod_{k=1}^{c} \frac{i+j+k-1}{i+j+k-2}.$$

6

**Lecture 2**

**The Aztec diamond**

The graphs $AD_n$ introduced towards the end of the previous lecture are called the *Aztec diamond* graphs. They were introduced by Elkies, Kuperberg, Larsen, and Propp, who proved in 1992 the following result.

THEOREM 2.1. *For all $n \geq 1$ we have*

$$\mathrm{M}(AD_n) = 2^{n(n+1)/2}. \tag{2.1}$$

The short proof we present here is based on the following two preliminary lemmas.

LEMMA 2.2 (VERTEX SPLITTING LEMMA). *Let $G$ be a graph, $v$ a vertex of it, and denote the set of neighbors of $v$ by $N(v)$. For an arbitrary partition $N(v) = H \cup K$, let $G'$ be the graph obtained from $G \setminus v$ by including three new vertices $v'$, $v''$, and $x$ so that $N(v') = H \cup \{x\}$, $N(v'') = K \cup \{x\}$, and $N(x) = \{v', v''\}$. Then*

$$\mathrm{M}(G) = \mathrm{M}(G'). \tag{2.2}$$

*Pictorially, we have*
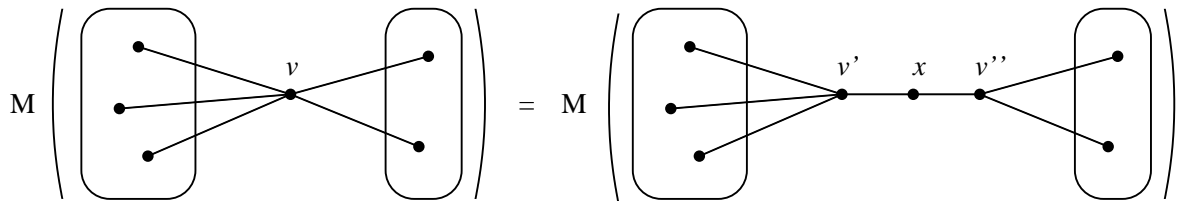


*Proof.* We set up a bijection between the set $\mathcal{M}(G)$ of perfect matchings of $G$ and the set $\mathcal{M}(G')$ of perfect matchings of $G'$. Given $\mu \in \mathcal{M}(G)$, look at the vertex $w$ matched up with $v$ under $\mu$. If $w \in H$, associate to $\mu$ the perfect matching of $G'$ in which $v'$ is matched to $w$, $x$ to $v''$, and all remaining vertices are matched up exactly as in $\mu$. If $w \in K$, associate to $\mu$ the perfect matching of $G'$ in which $v''$ is matched to $w$, $x$ to $v'$, and all remaining vertices are matched up exactly as in $\mu$. It is readily checked that this correspondence is a bijection. $\square$

In the next lemma graphs with weights on the edges appear. For such a weighted graph $G$ we denote by $\mathrm{M}(G)$ the *weighted count* of its perfect matchings, i.e. the sum of the weights of its perfect matchings, where the weight of a perfect matching is defined to
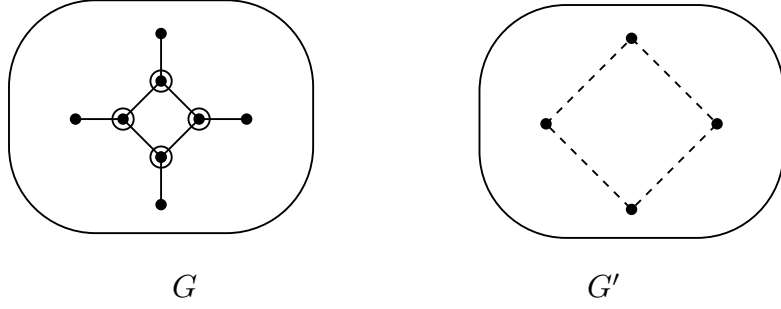
$$G \qquad\qquad G'$$

FIGURE 2.1. Illustration of the Spider lemma; dashed lines indicate edges weighted 1/2; circled vertices indicate vertices that have no other neighbors besides the ones shown.

be the product of the weights of the edges in it (note that this specializes to the number of perfect matchings if all edge weights are chosen to be 1).

LEMMA 2.3 (SPIDER LEMMA). *Let $G$ be a graph which contains the local configuration shown on the left of Figure 2.1, i.e. it contains a 4-cycle $C$ whose vertices have degree 3 in $G$, so that the four vertices outside $C$ that have a neighbor in $C$ are distinct. Let $G'$ be the graph obtained from $G$ by deleting the vertices of $C$ and including four new edges, each weighted by 1/2, as indicated on the right of Figure 2.1. Then we have*

$$\mathrm{M}(G) = 2\,\mathrm{M}(G'). \qquad\qquad (2.3)$$

*Proof.* Let $N$ be the set consisting of the four vertices of $G$ outside $C$ that have neighbors in $C$ (i.e., $N$ consists of the four outer vertices in the pattern shown in Figure 2.1). Partition the set of perfect matchings of $G$ and $G'$ according to the subsets of $N$ which are matched outside $C \cup N$. All such subsets of $N$ necessarily have even size (indeed, and odd such subset of $N$ would leave an odd number of vertices in our patterns to be matched among themselves, which is impossible). The possible situations are illustrated in Figure 2.2 (note that when the subset of externally matched vertices of $N$ has size two, the neighbors in $C$ of these two vertices must be adjacent, otherwise the leftover portions of our patterns have no perfect matchings). The numbers below each figure represent the total weight of the perfect matchings of the leftover portions of our local patterns. For instance, in the top left figure the portion of our local pattern that is still to be covered is a 4-cycle, so it has two perfect matchings; in the middle row, in the picture on the right there is just one way to match the leftover two vertices, and that matching has weight 1/2. Since in all instances the number on the left is precisely twice the number on the right, the statement follows. □

*Proof of Theorem 2.1.* Consider the following sequence of graphs that starts with $AD_n$ and ends with $AD_{n-1}$ (the figure illustrates the case $n = 4$, but all details are the same in the general case). Let us keep track how the number of perfect matchings changes when we go from each graph in the sequence to the next.

From the first to the second, the number of perfect matchings stays unchanged, by repeated application of the vertex splitting lemma (Lemma 2.1). Next we apply the
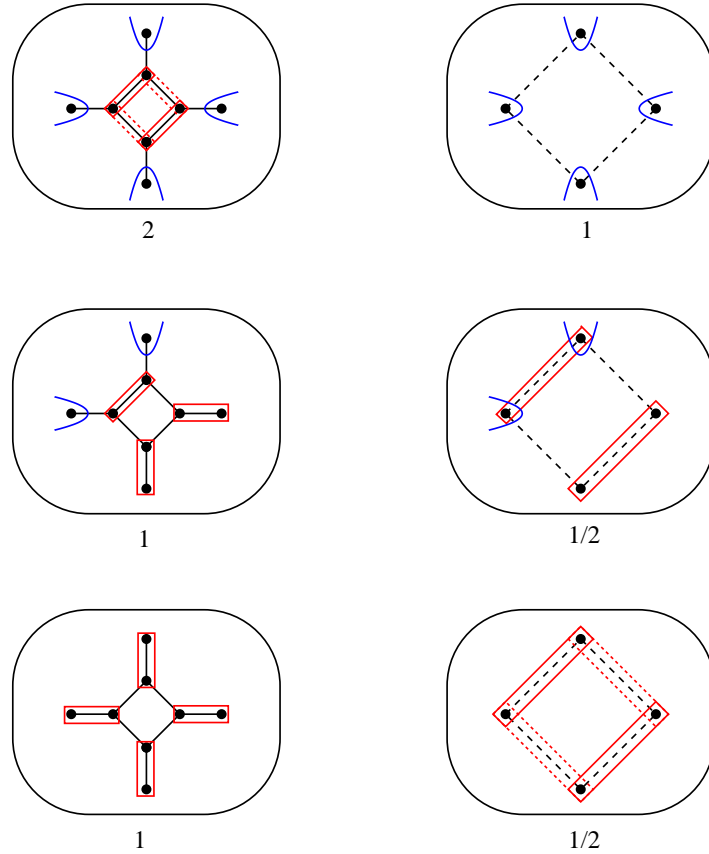
FIGURE 2.2

spider lemma in the places indicated on the third graph. Thus when we arrive at the fourth graph, we pick up a factor of $2^{n^2}$; the dashed edges indicate edges weighted by $1/2$. Next a key point happens: when we delete the forced edges (i.e., edges that are forced to be part of any perfect matching) in the fourth graph, what we are left with is $AD_{n-1}$, with all edges weighted $1/2$ (note that all forced edges had weight 1, so their removal leaves the weighted count of perfect matchings unchanged). To connect back to $AD_{n-1}$ with unit weights on edges, note that each perfect matching of $AD_{n-1}$ has $n(n-1)$ edges in it (this is half the number of vertices of $AD_{n-1}$). Thus the weighted count of matchings of $AD_{n-1}$ with weights $1/2$ everywhere equals $\frac{1}{2^{n(n-1)/2}} \, \mathrm{M}(AD_{n-1})$. Putting all this together we obtain

$$M(AD_n) = 2^n \, \mathrm{M}(AD_{n-1}), \tag{2.4}$$

which when applied repeatedly implies (2.1). □

We have seen that the vertex splitting lemma and the spider lemma fit together nicely to afford the above proof of Theorem 2.1. It turns out they have weighted extensions that allow one to prove a much more general result — namely, a version of (2.4) with *arbitrary weights* on the edges of $AD_n$ (see the "Reduction Theorem" of the next lecture). (It is interesting to note that even for graphs with all edge weights equal to 1, the statement of the spider lemma involves, in the graph $G'$, some weights different from 1.)
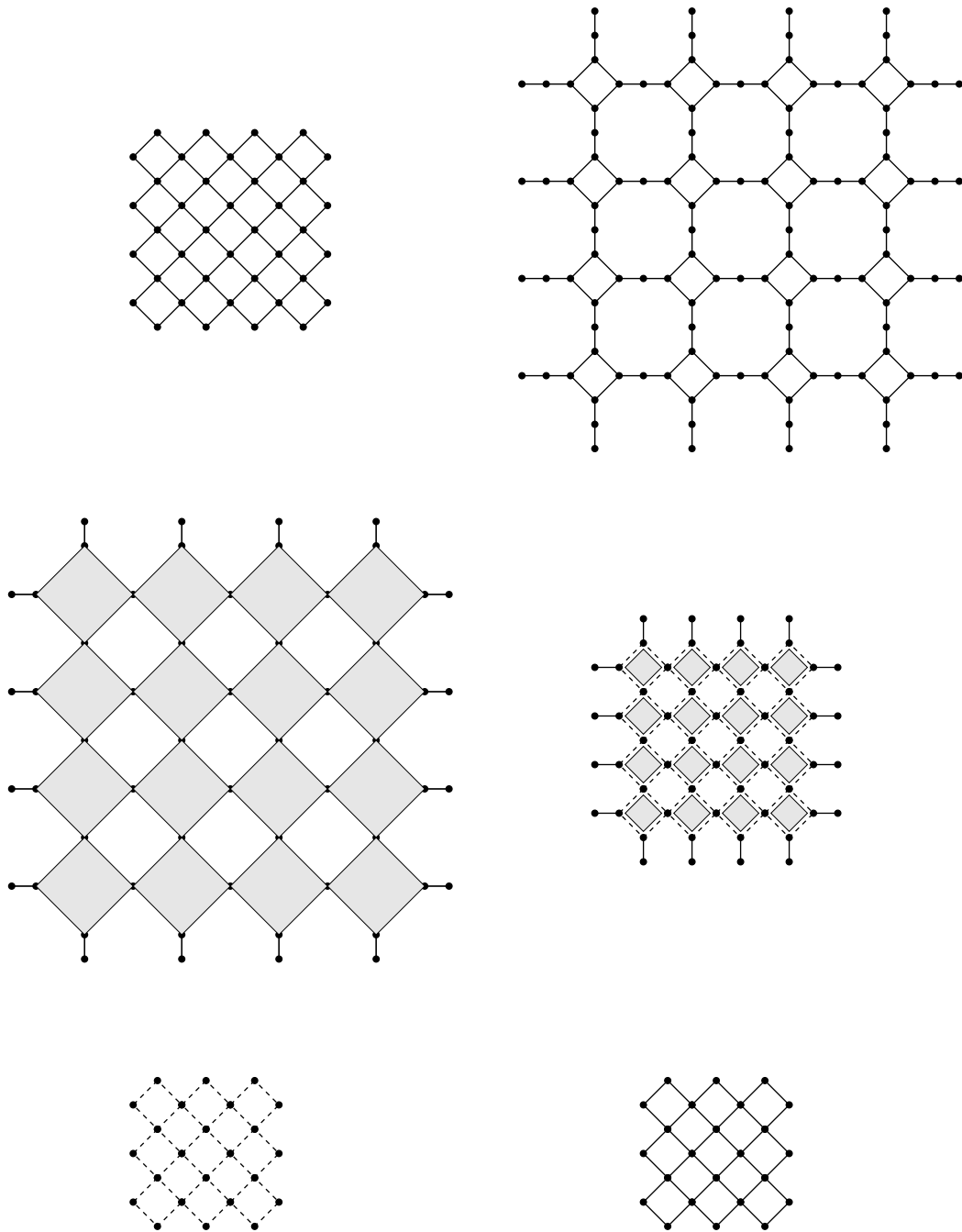
The vertex splitting lemma readily extends to the weighted case.

LEMMA 2.4 (WEIGHTED VERTEX SPLITTING LEMMA). *Let $G$ be a weighted graph, and construct the weighted graph $G'$ from it as follows. Take the structure of $G'$ to be exactly that defined in Lemma 2.1. Define the weights of edges $\{x, v'\}$ and $\{x, v''\}$ to be 1, and the weights of all remaining edges of $G'$ to be the same as they were in $G$. Then $\mathrm{M}(G) = \mathrm{M}(G')$.*
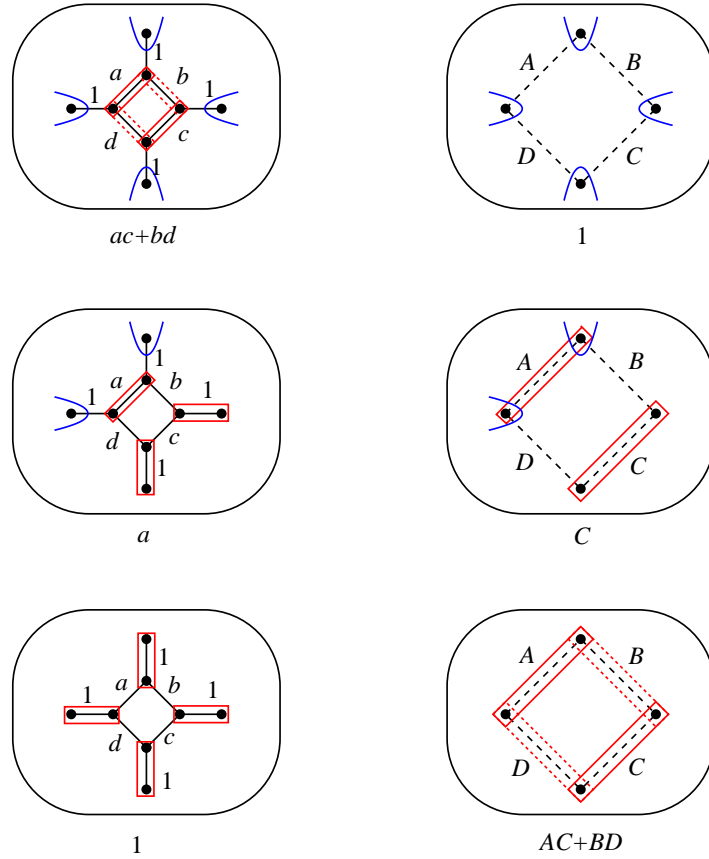
10

FIGURE 2.3

*Proof.* It is readily checked that, due to the choice of the edge weights in $G'$, the bijection between $\mathcal{M}(G)$ and $\mathcal{M}(G')$ described in the proof of Lemma 2.2 is weight preserving. This implies the statement. □

To extend the spider lemma we need a little more work, but the ideas are the same.

LEMMA 2.5 (WEIGHTED SPIDER LEMMA). *Let $G$ be a weighted graph which contains the local configuration shown on the left of Figure 2.1, and suppose the weights of the edges in the 4-cycle $C$ are (clockwise from top left) $a$, $b$, $c$, and $d$, while the weights of the four other edges incident to $C$ are 1. Let $G'$ have the structure described in Lemma 2.3, with the weights of the shown 4-cycle in $G'$ be (clockwise from top left) $c/(ac+bd)$, $d/(ac+bd)$, $a/(ac+bd)$, and $b/(ac+bd)$, and all other edge weights the same as in $G$. Then we have*

$$\mathrm{M}(G) = (ac+bd)\,\mathrm{M}(G'). \tag{2.5}$$

*Proof.* Rather then simply checking that the specified weights work, let us deduce them. Denote by $A$, $B$, $C$, and $D$ the weights of the 4-cycle of $G'$ displayed in Figure 2.3. Our goal is to choose them in such a way that the reasoning in the proof of Lemma 2.3 leads to two columns of weights that are proportional. These weights are readily seen to be as indicated in Figure 2.3; note that there are three more cases analogous to the one

11

pictured in the middle, where the weights of the selected edge on the left are $b$, $c$, and $d$, respectively. Imposing the condition that the two columns of weights are proportional, and denoting the constant of proportionality by $k$, we obtain the following six equations:

$$ab + cd = k$$
$$a = kC$$
$$b = kD$$
$$c = kA$$
$$d = kB$$
$$1 = k(AC + BD).$$

The first five of these yield $k = ac + bd$, $A = c/(ac+bd)$, $B = d/(ac+bd)$, $C = a/(ac+bd)$, and $D = b/(ac+bd)$. It is readily checked that these values also satisfy the sixth equation. This completes the proof. □

# Lecture 3

## The Reduction Theorem and fortress graphs

We present now the extension of (2.4) to Aztec diamond graphs with arbitrary weights on their edges.

Let wt be an arbitrary weight function on the edges of $AD_n$. We construct a new weight wt' on the edges of $AD_{n-1}$ as follows. Regard $AD_n$ as being composed of $n^2$ "cells" — the $n^2$ 4-cycles into which its edges can be partitioned. Change the weight on each cell of $AD_n$ as indicated in Figure 3.1[1]:
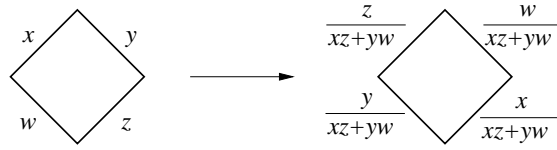


FIGURE 3.1

Then take the restriction of the resulting weight on $AD_n$ to the graph isomorphic to $AD_{n-1}$ that can be seen "in the middle" of $AD_n$ (see Figure 3.2):
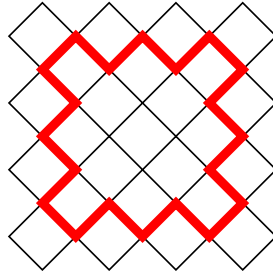


FIGURE 3.2

This is the weight wt' on $AD_{n-1}$ we wanted to construct. Let $\mathcal{C}$ be the set of cells of $AD_n$. If a cell $c$ has its four edge weights $x$, $y$, $z$, and $w$ (in cyclic order), we define the *cell factor* $\Delta(c)$ to be $\Delta(c) := xz + yw$.

THEOREM 3.1 (REDUCTION THEOREM). *For all $n \geq 1$ and for any weight function* wt *on the edges of $AD_n$, the weight* wt' *on $AD_{n-1}$ defined above is such that*

$$\mathrm{M}(AD_n; \mathrm{wt}) = \left(\prod_{c \in \mathcal{C}} \Delta(c)\right) \mathrm{M}(AD_{n-1}; \mathrm{wt}').  \tag{3.1}$$

---

[1]We assume here that all resulting denominators in Figure 3.1 are different from 0. This is always the case if for instance the edge weights are regarded as indeterminates. In concrete numerical examples it may happen that the weights on some cells produce a denominator equal to 0; such instances require special attention.

*Proof.* Follow the same arguments we gave in the proof of Theorem 2.1 in Lecture 2, but instead of Lemmas 2.2 and 2.3 use their weighted generalizations given in Lemmas 2.4 and 2.5, respectively. The product on the right hand side of (3.1) arises due to the $n^2$ applications of the weighted spider lemma (Lemma 2.5). The shuffling of the weights prescribed by the latter, and the fact that the fifth graph in the proof of Theorem 2.1 ($AD_{n-1}$) was obtained by deleting the vertices of the "outer ring" of the first graph in the proof of Theorem 2.1 ($AD_n$), causes the resulting weight on $AD_{n-1}$ to be precisely the weight wt$'$ defined above. $\square$

As a first application of this extension of Theorem 2.1, we consider a new family of graphs, called *fortress graphs.* Their definition is apparent by looking at the first few graphs in this family, as shown in Figure 3.3.
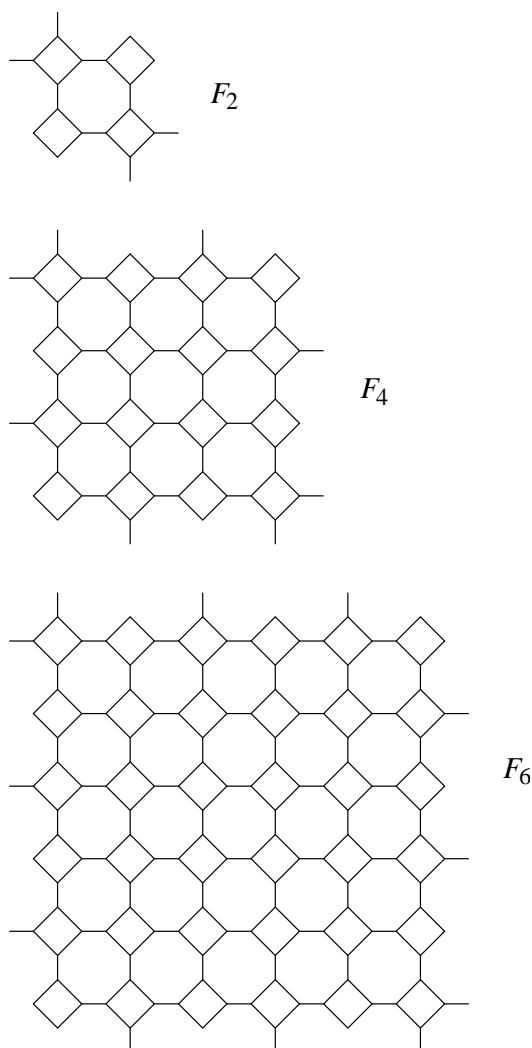


$F_2$

$F_4$

$F_6$

FIGURE 3.3

In general, $F_{2n}$ consists of $(2n)^2$ 4-cycles joined together by edges, with extra pending edges added along the perimeter according to the rule shown in Figure 3.3.

As in the case of Aztec diamonds, the number of perfect matchings of $F_{2n}$ also turns out to be a perfect power. But the base is different.

THEOREM 3.2. *For all $n \geq 1$ we have*

$$M(F_{2n}) = 5^{n^2}. \tag{3.2}$$

*Proof.* In the graph $F_{2n}$ there are $n^2$ opportunities to apply the spider lemma (Lemma 2.3); these locations are indicated in Figure 3.4 in the case $n = 2$. Apply the spider lemma at all these places. Note that the resulting graph is $AD_{2n}$, with edges weighted by 1 or 1/2, as resulting from the $n^2$ applications of the spider lemma (for $n = 2$, this is pictured in Figure 3.5; as indicated there, solid lines denote weights equal to 1, and dotted lines weights equal to 1/2); denote this weight function by $\mathrm{wt}_1$. We obtain
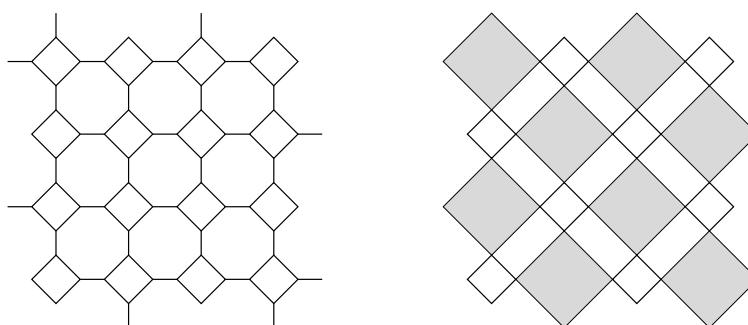


FIGURE 3.4
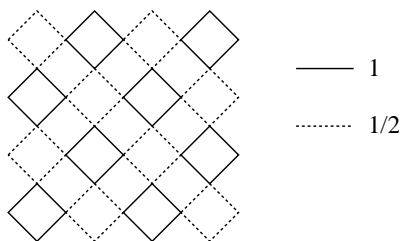


FIGURE 3.5

$$M(F_{2n}) = 2^{n^2} M(AD_{2n}; \mathrm{wt}_1). \tag{3.3}$$

Apply the Reduction Theorem to the graph on the right hand side above. Since the cells with edges weighted by 1 contribute cell factors of 2, and those whose edges are weighted by 1/2 produce cell factors of $\frac{1}{2} \cdot \frac{1}{2} + \frac{1}{2} \cdot \frac{1}{2} = \frac{1}{2}$, this yields

$$M(AD_{2n}; \mathrm{wt}_1) = 2^{2n^2} \left(\frac{1}{2}\right)^{2n^2} M(AD_{2n-1}; \mathrm{wt}_2), \tag{3.4}$$

15

FIGURE 3.6



FIGURE 3.7

where the weight $wt_2$ is obtained from $wt_1$ by the procedure illustrated in Figures 3.1–3.2; in the case of our weights, these figures take the forms shown in Figures 3.6–3.7 (i.e., the thick contour in Figure 3.7 contains $AD_{2n-1}$ weighted by $wt_2$, for $n = 2$).

At this point we start seeing how this proof might be finished. Had the resulting weight $wt_2$ be the same (or equivalent to) $wt_1$, the equations above would have impli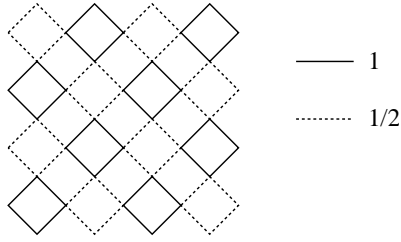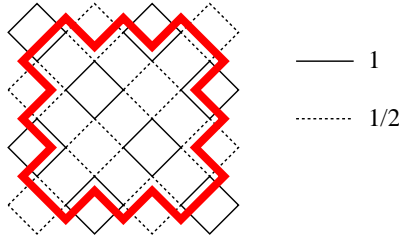ed a recurrence relation that would have solved the problem. This is not the case, but we can apply the reduction theorem again, for a new chance of this idea to work. Plugging in the values of our weights in Figure 3.1, we see that this second application of the Reduction Theorem gives (see Figure 3.8)
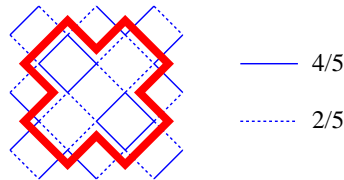


FIGURE 3.8

$$\mathrm{M}(AD_{2n-1}; wt_2) = \left(\frac{5}{4}\right)^{(2n-1)^2} \mathrm{M}(AD_{2n-2}; wt_3), \tag{3.5}$$

where $wt_3$ is the weight described in Figure 3.8. After reflecting $wt_3$ across the vertical symmetry axis of $AD_{2n-2}$, it becomes proportional to $wt_1$ (more precisely, 4/5 times $wt_1$). Since each perfect matching of $AD_{2n-2}$ contains exactly $(2n-2)(2n-1)$ edges, we see that the hope expressed in the previous paragraph is fulfilled, as we get

$$\mathrm{M}(AD_{2n-2}; wt_3) = \left(\frac{4}{5}\right)^{(2n-2)(2n-1)} \mathrm{M}(AD_{2n-2}; wt_1). \tag{3.6}$$

16

Replacing now $n$ by $n-1$ in (3.3) gives

$$\mathrm{M}(AD_{2n-2}; wt_1) = \left(\frac{1}{2}\right)^{(n-1)^2} \mathrm{M}(F_{2n-2}). \qquad (3.7)$$

Putting together equations (3.3)–(3.7) we obtain

$$\mathrm{M}(F_{2n}) = 5^{n^2} \mathrm{M}(F_{2n-2}).$$

Applying this repeatedly one obtains (3.2). $\qquad\square$

# Lecture 4

## A unifying point of view and a new problem suggested by it: Aztec dungeons

Our consideration of fortress graphs in the previous lecture may look a little arbitrary. There is however a very simple but quite useful fact that can help motivate the definition of fortresses. This fact is that often perfect matchings problems can be equivalently phrased as *tiling problems*. For instance, suppose we are given a lattice $\mathcal{L}$ in the plane, and a finite lattice region $R$ on it. Define a *tile* to be the union of any two fundamental regions of $\mathcal{L}$ which share an edge. A *tiling* of $R$ is by definition a complete covering of $R$ with such non-overlapping tiles.

Now let $G := R^*$ be the *dual graph* pf $R$, i.e. the graph whose vertices are fundamental regions of $\mathcal{L}$ contained in $R$, and whose edges connect those pairs of vertices which correspond to fundamental regions that share an edge. Then by construction the perfect matchings of $G$ can be identified with tilings of $R$. Figure 4.1 illustrates the domino tiling corresponding to a perfect matching of $AD_2$.
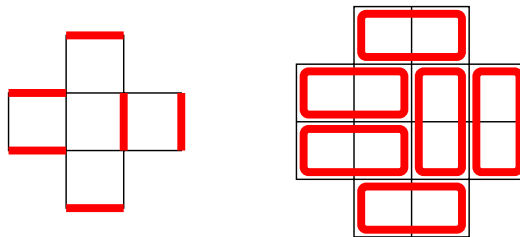


FIGURE 4.1

With this in mind, note that the Aztec diamond graphs are obtained by starting with the square lattice, and taking duals of regions like the one shown in Figure 4.2.



FIGURE 4.2

18
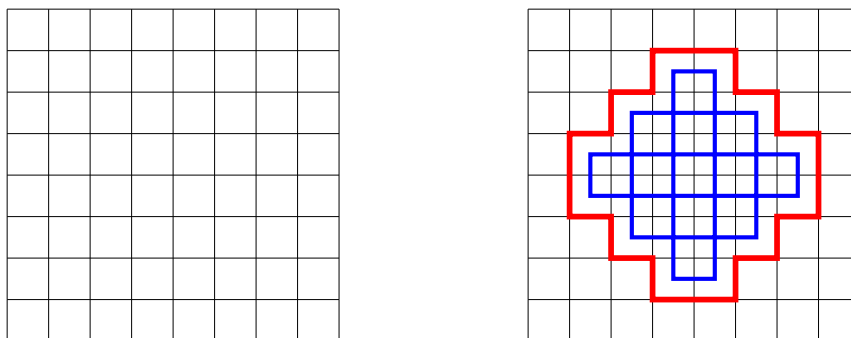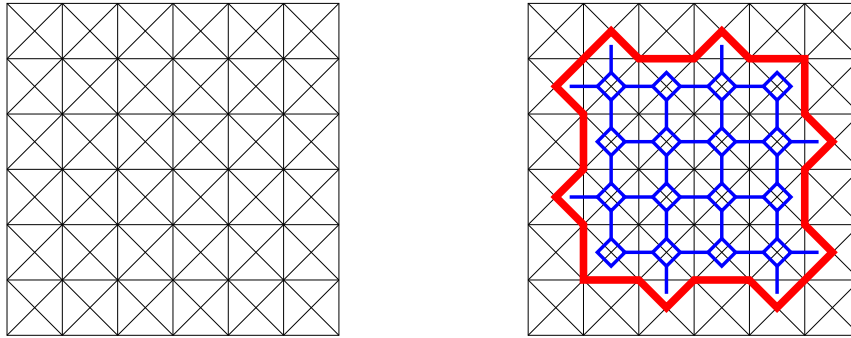
FIGURE 4.3

On the other hand, the fortress graphs are are obtained by starting with the lattice obtained from the square lattice by drawing in both diagonals in each unit lattice square, and taking duals of regions like the one shown in Figure 4.3.

How about the triangular lattice? No family of lattice regions on the triangular lattice seems to be known whose number of tilings is analogous to the power of 2 and power of 5 formulas that we have seen in the previous lectures[2]. However, on the lattice obtained from the triangular lattice by drawing in all altitudes in each unit triangle, there is such a family of regions.
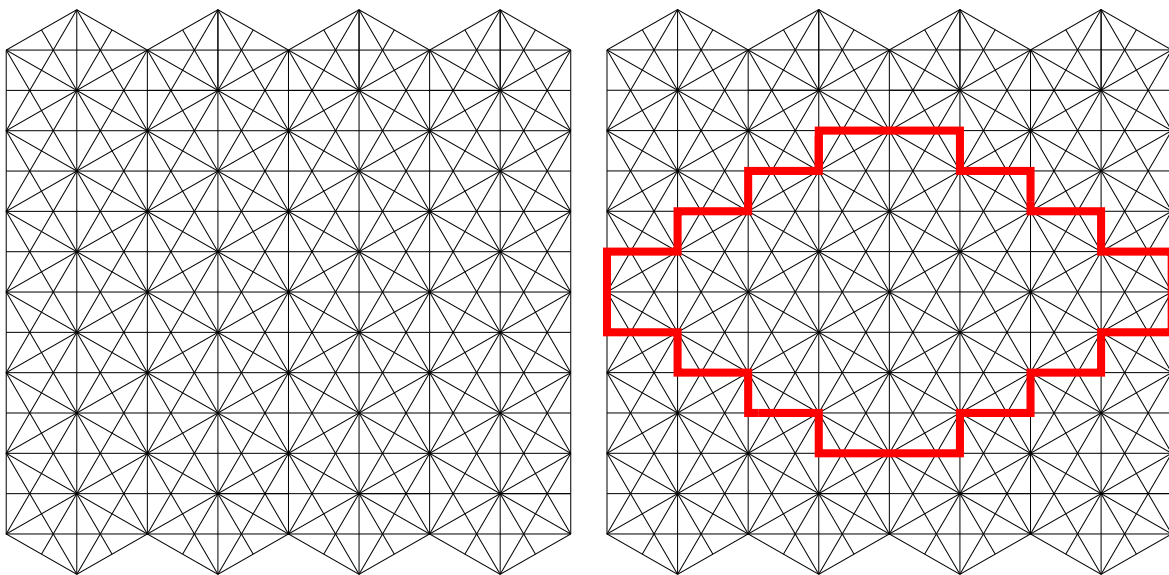


FIGURE 4.4

Namely, take a contour on this lattice in the shape of a slightly squashed Aztec diamond, as shown in Figure 4.4. If the chosen contour is the Aztec diamond of order $n$,

---

[2]Note that MacMahon's theorem (Theorem 1.2) does have a nice translation in terms of tilings on the triangular lattice (more precisely, unit rhombus tilings of hexagonal regions on the triangular lattice), but the resulting formula is not a perfect power.

define the dual of the obtained lattice region to be the *Aztec dungeon of order $n$*, and denote it by $D_n$ ($D_4$ is illustrated in Figure 4.5). The number of perfect matchings of $D_n$ again turns out to be (up to a possible multiple of two) a perfect power — this time with base 13.

THEOREM 4.1. *The number of perfect matchings of the Aztec dungeon $D_n$ is given by the equalities* $\mathrm{M}(D_0) = 1$, $\mathrm{M}(D_1) = 2$, $\mathrm{M}(D_2) = 13$, $\mathrm{M}(D_3) = 13^3$, $\mathrm{M}(D_4) = 2 \cdot 13^5$, $\mathrm{M}(D_5) = 13^8$, *and for $n \geq 5$ by the recurrence*

$$\mathrm{M}(D_{n+1}) = 13^{4n-8}\,\mathrm{M}(D_{n-5}). \tag{4.1}$$

The proof of Theorem 4.1 will follow from the following three preliminary results. The first of them expresses $\mathrm{M}(D_n)$ in terms of a certain weighted count of perfect matchings of the Aztec diamond graph $AD_{2n-2}$.

Let $A$ be a given $k \times l$ matrix with $k$ and $l$ even. The centers of the edges of the Aztec diamond graph $AD_n$ form a $2n \times 2n$ array. Place a copy of $A$ in the upper left corner of this array and fill in the rest of the array periodically with period $A$ (i.e., translate $A$ to the right in the array $l$ units at a time and down in the array $k$ units at a time; if $2n$ is not a multiple of $k$ or $l$ some of these translates will fit only partially in the array).

DEFINITION 4.2. *Define the weight* $\mathrm{wt}_A$ *on the edges of $AD_n$ by assigning each edge the corresponding entry of $A$ in the array described above.*

LEMMA 4.3. *Let $N$ be the matrix*

$$N = \begin{bmatrix} \frac{1}{2} & 1 & 1 & \frac{1}{2} \\ 1 & 0 & 1 & 1 \\ 1 & 1 & 0 & 1 \\ \frac{1}{1} & 1 & 1 & \frac{1}{2} \end{bmatrix}. \tag{4.2}$$

*We have*

$$\mathrm{M}(D_n) = 2^{n^2}\,\mathrm{M}(AD_{2n-2}; \mathrm{wt}_N). \tag{4.3}$$

*Proof.* Consider the graph $D_n$ (this is illustrated in Figure 4.5 for $n = 4$). This graph contains many local configurations like the one in the statement of the spider lemma (Lemma 2.3), providing one with as many opportunities to apply it. By their geometric orientation, these local configurations can be grouped into three families. The largest family contains $n^2$ members (these are indicated in Figure 4.6). Apply the spider lemma at each of these $n^2$ places. The resulting weighted graph is readily seen to be isomorphic with a weighted subgraph of the square lattice (shown in Figure 4.7 for $n = 4$).

Furthermore, because of the vertices of degree one, the resulting subgraph of the square lattice will have some edges around the boundary that are forced to be contained in all of its perfect matchings (the forced edges are shown in thick lines in Figure 4.7).

Removing all vertices (together with all incident edges) connected by forced edges we are left with a weighted spanning subgraph of the Aztec diamond of order $2n - 2$ (Figure

20
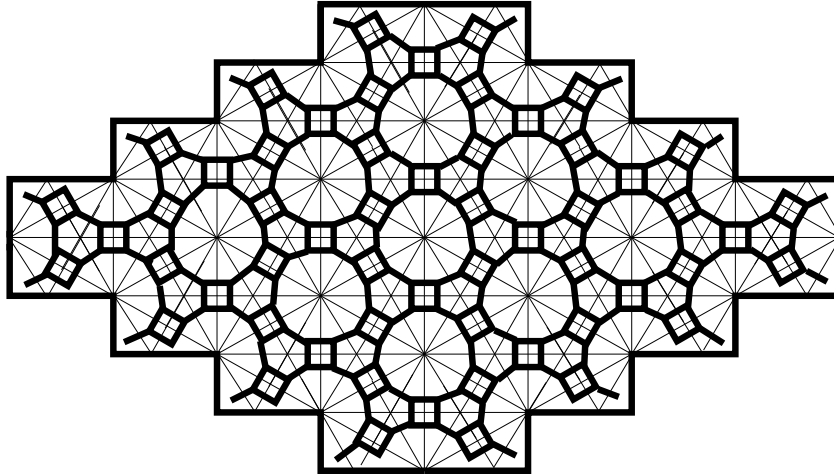
FIGURE 4.5. The Aztec dungeon $D_4$ and its dual graph.
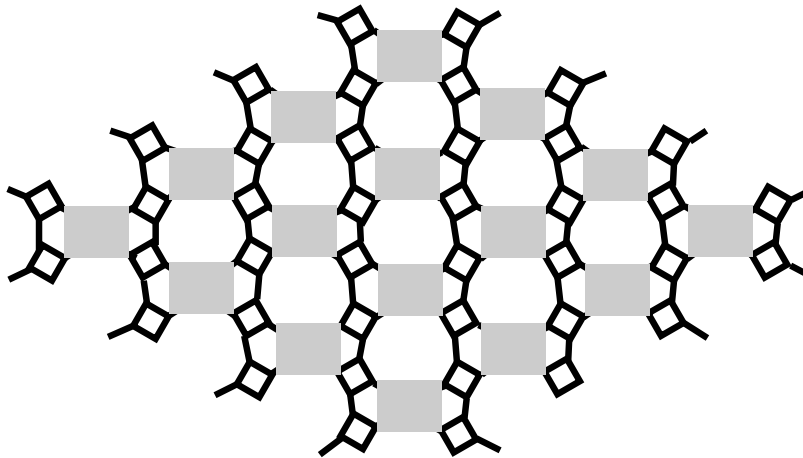


FIGURE 4.6. Applying Lemma 2.3 to the graph dual to $D_4$.

4.8 illustrates the case $n = 4$; the thick edges have weight $1/2$). This can be regarded as the entire graph $AD_{2n-2}$ by weighting all missing edges by 0. By the spider lemma, the obtained weight comes out to be exactly $\text{wt}_N$, with the matrix $N$ given by (4.2). This implies (4.3). $\qquad\square$

For a $k \times l$ matrix $A$ with $k$ and $l$ even define a new $k \times l$ matrix $\mathrm{d}(A)$ as follows. Divide matrix $A$ into $2 \times 2$ blocks

$$\begin{bmatrix} x & w \\ y & z \end{bmatrix}$$

and assume $xz + yw \neq 0$ for all such blocks. Replace each such block by

$$\begin{bmatrix} z/(xz + yw) & y/(xz + yw) \\ w/(xz + yw) & x/(xz + yw) \end{bmatrix}$$

and denote the resulting $k \times l$ matrix by $B$. Define $\mathrm{d}(A)$ to be the $k \times l$ matrix obtained from $B$ by cyclically shifting its columns one unit up and cyclically shifting the rows of the resulting matrix one unit to the left.

21

FIGURE 4.7. A graph embedded in $\mathbb{Z}^2$.    FIGURE 4.8. A weight on $AD_6$.

The next simple observation provides a convenient way of keeping track of the evolution of periodic weights on Aztec diamonds when one applies the Reduction Theorem.

LEMMA 4.4. *Let $A$ be a $k \times l$ matrix with $k$ and $l$ even and consider the weight $\mathrm{wt}_A$ it determines on $AD_n$ according to Definition 4.2. When applying the Reduction Theorem to $AD_n$ weighted by $\mathrm{wt}_A$, the resulting weight on $AD_{n-1}$ is $\mathrm{wt}_{\mathrm{d}(A)}$, where $\mathrm{d}$ is the matrix operator defined above.*

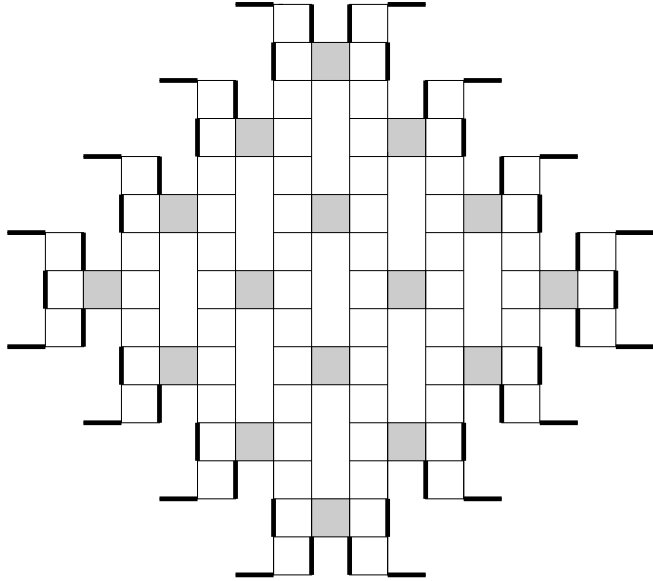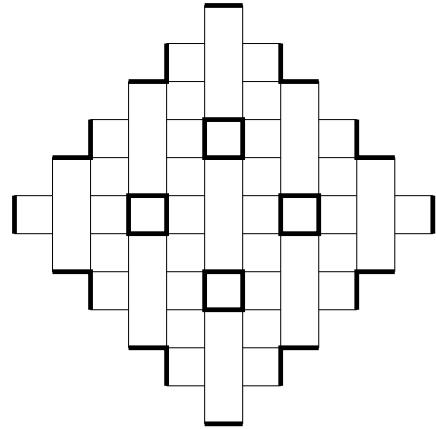*Proof.* This follows from the Reduction Theorem and the above construction of $\mathrm{d}(A)$. The reason we need the cyclic shifts in the construction of $\mathrm{d}(A)$ is because on the right hand side of (3.1) the Aztec diamond of order $n-1$ is viewed as being embedded concentrically into the Aztec diamond of order $n$ on the left hand side in (3.1), while the weight $\mathrm{wt}_B$ is defined by fitting $B$ into the upper left corner of the array formed by the midpoints of the edges of each Aztec diamond.  $\square$

Due to the location of the 0's in the matrix $N$ given by (3.2), all the edges in an Aztec diamond that are weighted 0 under $\mathrm{wt}_N$ are parallel among themselves. By the pattern in Figure 3.1, this property is preserved whenever we apply the Reduction Theorem. In particular, in any cell at least one pair of opposite edges is assigned nonzero weights. Therefore all cell-factors are nonzero and the Reduction Theorem can be applied successively.

By Lemma 4.4, the successive weights that occur are the weights corresponding via Definition 4.2 to the iterates $\mathrm{d}^{(i)}(N)$, for $i = 1, 2, 3, \ldots$. Therefore, if one of these iterates would be the same as $N$—or the same up to a scalar multiplicative factor—then we would get a recurrence for the number of perfect matchings on the right hand side of (4.3). By (4.3) this would then translate into a recurrence for $\mathrm{M}(D_n)$ and would solve the problem of computing the latter.

The computation of the iterates $\mathrm{d}^{(i)}(N)$ can be done very easily with a computer alge-

22

bra package like Maple. The first few iterates don't look very promising, but perseverance pays off: the twelfth(!) iterate turns out to be, up to a scalar multiple, exactly the same as $N$. More precisely, one obtains

$$\mathrm{d}^{(12)}(N) = k_0 N, \tag{4.4}$$

with

$$k_0 = \frac{3^4 \cdot 5^4}{2^4 \cdot 13^4}. \tag{4.5}$$

Since at each application of the Reduction Theorem the order of the resulting Aztec diamond decreases one unit, it follows that

$$\mathrm{M}(AD_{2n}; \mathrm{wt}_N) = k_1 \mathrm{M}(AD_{2n-12}; \mathrm{wt}_N), \tag{4.6}$$

where the constant $k_1$ is the product of all the cell-factors arising in the twelve applications of the Reduction Theorem, multiplied by $k_0^{(2n-12)(2n-11)}$ (the latter factor is due to (4.4) and to the fact that each perfect matching of $AD_n$ contains $n(n+1)$ edges). To carry out the computation of $k_1$ by hand would be fairly strenuous, but with the assistance of Maple it is quite easy. We obtain by (4.6) the following result.

PROPOSITION 4.5. *For $n \geq 6$ we have*

$$\mathrm{M}(AD_{2n}; \mathrm{wt}_N) = 2^{24-12n} 13^{4n-8} \mathrm{M}(AD_{2n-12}; \mathrm{wt}_N). \tag{4.7}$$

We are now ready to present the proof of the enumeration of perfect matchings of the Aztec dungeons.

*Proof of Theorem 4.1.* By Lemma 4.3 we have

$$\mathrm{M}(D_{n+1}) = 2^{(n+1)^2} \mathrm{M}(AD_{2n}; \mathrm{wt}_N)$$

and

$$\mathrm{M}(D_{n-5}) = 2^{(n-5)^2} \mathrm{M}(AD_{2n-12}; \mathrm{wt}_N).$$

Together with (4.7) these two equalities imply (4.1). The stated values for the number of perfect matchings of the first six Aztec dungeons are easily checked using (4.3) and applying repeatedly the Reduction Theorem to evaluate the weighted perfect matching counts of the resulting Aztec diamonds. □

## Lecture 5

## An extension of the Reduction Theorem and a new class of graphs it suggests

The main idea we have seen so far is contained in the Reduction Theorem. It turns out that one can generalize this from weighted Aztec diamond graphs to a larger class of graphs, which we describe next.

A *cellular graph* is a graph $G$ defined as follows:

($i$) a *cell* is a 4-cycle
($ii$) $G$ is a union of cells that can have common vertices
($iii$) at each vertex of $G$ at most two cells meet.

Let $G$ be a cellular graph with an arbitrary weight function on its edges. Group the cells of $G$ in "lines of cells" as follows. Let $H$ be the graph whose vertex set is the same as the vertex set of $G$, with two vertices being connected by an edge in $H$ if and only if they are opposite vertices in the same cell. Due to condition ($iii$) above, the edge set of $H$ is naturally partitioned into a union of disjoint maximal (possibly closed) paths. Call the cells along such a maximal path of $H$ a *line of cells*. Call the vertices of $G$ that are endpoints of maximal paths in $H$ *extremal vertices* (these are precisely those vertices of $G$ that belong to a single cell).
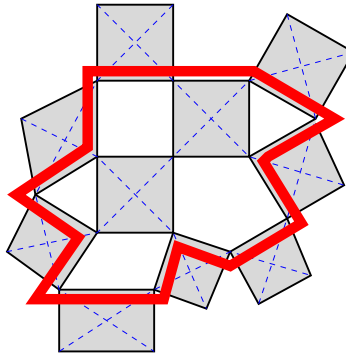


Figure 5.1. An example of a cellular graph $G$ and the corresponding graph $G'$.

Given a cellular graph $G$ with an arbitrary weight function wt on its edges, define $G'$ to be the subgraph of $G$ induced by its non-extremal vertices (Figure 5.1 shows an example; the cells of $G$ are shaded, $G'$ is the subgraph induced by the vertices inside the thick contour), and weight the edges of $G'$ by a new weight wt$'$ defined as follows: apply the rule shown in Figure 3.1 in each cell of $G$, and then restrict the resulting weight to the edges of $G'$. Recall that for a cell $c$ with weights $x$, $y$, $z$, $w$ on its edges (in cyclic order) the cell factor $\Delta(c)$ is $\Delta(c) = xz + yw$.

The generalization of the reduction Theorem we referred to above is the following (see [**2**] for the proof).
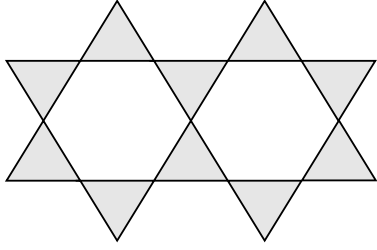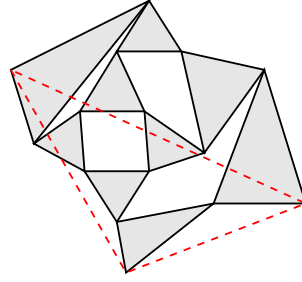
FIGURE 5.2. A tricellular graph.



FIGURE 5.3. A 4-regular tricellular graph.

THEOREM 5.1. *Let $G$ be a cellular graph with an arbitrary weight function* wt *on its edges. Let $\mathcal{C}$ be the set of cells of $G$. Then if $G'$ and* wt$'$ *are defined as above, we have*

$$\mathrm{M}(G; \mathrm{wt}) = \left( \prod_{c \in \mathcal{C}} \Delta(c) \right) \mathrm{M}(G'; \mathrm{wt}'). \tag{5.1}$$

In the above definition of a cellular graph, choosing cells to be 4-cycles may seem a little arbitrary. What if we look at graphs consisting of *triangular cells*? Can we say something about their number of perfect matchings? It turns out that the answer to this question is in the affirmative.

Define *tricellular graphs* by the same definition we used above for cellular graphs, with the sole modification that cells are now 3-cycles, i.e. replace ($i$) by

($i'$) a *cell* is a 3-cycle

and keep ($ii$) and ($iii$) unchanged. Figure 5.2 illustrates an example of a tricellular graph.

A graph is call *k-regular* if there are $k$ edges incident to each of its vertices. Figure 5.3 shows an example of a tricellular graph which is also 4-regular (the dotted lines are the edges of a cell which has not been shaded for clarity). It turns out that in such graphs the number of perfect matchings is determined by the number of vertices. We have the following result.

THEOREM 5.2. *Let $G$ be a 4-regular tricellular graph. Then the number of perfect matchings of $G$ is given by*

$$\mathrm{M}(G) = 2^{\frac{|V(G)|}{3}+1}. \tag{5.2}$$

A related kind of graphs, called *3-regular terminal graphs*, are graphs $G$ for which

• $V(G)$ is a disjoint union of vertices of triangular cells
• $E(G)$ consists of the edges of the triangular cells, plus some edges connecting vertices of different cells
• $G$ is 3-regular

An example of a 3-regular terminal graph is shown in Figure 5.4.

THEOREM 5.3. *Let $G$ be a 3-regular terminal graph. Then*

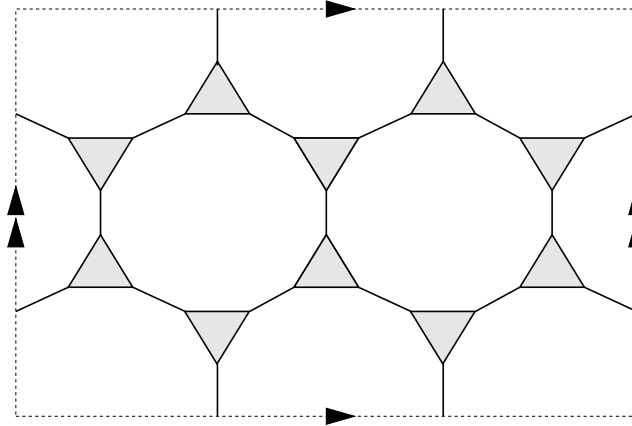$$\mathrm{M}(G) = 2^{\frac{|V(G)|}{6}+1}. \tag{5.3}$$

25

Figure 5.4. A 3-regular terminal graph embedded in the torus.

We will prove Theorem 5.3 first. It will imply Theorem 5.2. We need two basic ideas in our proof. The first one involves the Ising model of statistical physics and a simple and elegant trick that physicists call its "high temperature expansion." The second idea is the Fisher construction which relates the Ising model to perfect matchings.

The Ising model is a classical model in statistical physics, and it can be described as follows. Let $G$ be a finite graph (it may help the reader to think of $G$ as a concrete graph, for instance the $n \times n$ grid graph on a torus; but all definitions and arguments that follow work for arbitrary graphs).

Let $N$ be the number of vertices (also called sites) of $G$, and label them by $1, 2, \ldots, N$. Assign the value $\sigma_i$ to vertex $i$, with $\sigma_i \in \{+1, -1\}$, for $i = 1, \ldots, N$. Such an assignment is called a *state* and is denoted by $\{\sigma\}$. The Ising model gives each such state a certain energy $E(\sigma)$. The probabilities of occurrences of different states are then defined by requiring them to depend in a certain way on these energies (see (5.6)). We motivate below the definition of energies $E(\sigma)$ employed by the Ising model.

$$+1 \text{———} +1 \qquad\qquad +1 \text{———} -1$$

$$-1 \text{———} -1 \qquad\qquad -1 \text{———} +1$$
$$\text{(a)} \qquad\qquad\qquad \text{(b)}$$

Figure 5.5.

Let $\{\sigma\}$ be a state. Note that as far as an edge is concerned, only the four possibilities shown in Figure 5.5 can happen. The two possibilities in Figure 5.5(a) have the same value at the endpoints of the edge, and the two in Figure 5.5(b) have opposite values. Suppose we want to favor the situation of identical endpoints. Recall from physics the basic fact that lower energy states have higher probability. Thus to make identical values at the endpoints of an edge more likely than opposite values, we need to give lower energy to the configurations in Figure 5.5(a) than to the ones in Figure 5.5(b). One of

26

the simplest choices that accomplishes this is to let edge $\{i,j\}$ have energy $-k\sigma_i\sigma_j$, where $k > 0$. Define then the energy of a state as the sum of the energies of its edges:

$$\text{Energy}(\{\sigma\}) := \sum_{\text{edges}\{i,j\}} -k\sigma_i\sigma_j. \tag{5.4}$$

Recall that by Boltzmann's law the probability of a state is proportional to the exponential of minus its energy:

$$\text{Probability}(\{\sigma\}) \sim e^{-\text{Energy}(\{\sigma\})}. \tag{5.5}$$

By (5.4) and (5.5) we are led to

$$\text{Probability}(\{\sigma\}) \sim \prod_{\text{edges}\{i,j\}} e^{k\sigma_i\sigma_j}, \tag{5.6}$$

which determines the probabilities of individual states. These are the probabilities used in the Ising model.

The main object of study in the Ising model is the *partition function*, defined as

$$Z := \sum_{\{\sigma\}} \prod_{\text{edges}\{i,j\}} e^{k\sigma_i\sigma_j}. \tag{5.7}$$

The *high temperature expansion* of the Ising model is a way of rewriting the partition function (5.7) as a sum over *even sub graphs* of $G$ (i.e., subgraphs in which every vertex degree is an even number).

Interestingly, the crucial idea in accomplishing this is the following very simple identity.

LEMMA 5.4. *For $\sigma_i, \sigma_j = \pm 1$, one has*

$$e^{k\sigma_i\sigma_j} = \cosh(k\sigma_i\sigma_j)(1 + \tanh(k)\sigma_i\sigma_j). \tag{5.8}$$

*Proof.* We have

$$
\begin{aligned}
e^{k\sigma_i\sigma_j} &= \frac{e^{k\sigma_i\sigma_j} + e^{-k\sigma_i\sigma_j}}{2} + \frac{e^{k\sigma_i\sigma_j} - e^{-k\sigma_i\sigma_j}}{2} \\
&= \cosh(k\sigma_i\sigma_j) + \sinh(k\sigma_i\sigma_j) \\
&= \cosh(k\sigma_i\sigma_j)(1 + \tanh(k\sigma_i\sigma_j)) \\
&= \cosh(k\sigma_i\sigma_j)(1 + \tanh(k)\sigma_i\sigma_j).
\end{aligned}
$$

Note that all the power of this sequence of equalities comes at the last equality sign, which holds due to the obvious fact that for $\sigma_i\sigma_j = \pm 1$ one has $\tanh(k\sigma_i\sigma_j) = \tanh(k)\sigma_i\sigma_j$. $\square$

Now use identity (5.8) to rewrite the partition function (5.7) as

$$Z = \sum_{\sigma_1=\pm 1,\ldots,\sigma_N=\pm 1} \prod_{\{i,j\}\in E(G)} \cosh(k\sigma_i\sigma_j)(1+\tanh(k)\sigma_i\sigma_j)$$

$$= (\cosh(k))^{|E(G)|} \sum_{\sigma_1,\ldots,\sigma_N=\pm 1} \prod_{\{i,j\}\in E(G)} (1+v\sigma_i\sigma_j), \qquad (5.9)$$

where $v := \tanh(k)$.

Expand the product in the summand above as a sum of $2^{|E(G)|}$ terms. Each such term is obtained by selecting either $1$ or $v\sigma_i\sigma_j$ in each of the $|E(G)|$ factors of the product in (5.9), and then multiplying together the selections we have made. Thus the terms in the expansion of the product are in bijection with subsets of the edge set $E(G)$: given a collection $H$ of edges of $G$, the corresponding term in the expansion of the product is

$$v^{|H|} \prod_{\{a,b\}\in E(H)} \sigma_a\sigma_b.$$

Thus we can write

$$\sum_{\sigma_1,\ldots,\sigma_N=\pm 1} \prod_{\{i,j\}\in E(G)} (1+v\sigma_i\sigma_j) = \sum_{\sigma_1,\ldots,\sigma_N=\pm 1} \sum_{H \text{ subgraph of } G} v^{|E(H)|} \prod_{\{a,b\}\in E(H)} \sigma_a\sigma_b$$

$$= \sum_{H \text{ subgraph of } G} v^{|E(H)|} \sum_{\sigma_1,\ldots,\sigma_N=\pm 1} \prod_{\{a,b\}\in E(H)} \sigma_a\sigma_b$$

$$= \sum_{H \text{ subgraph of } G} v^{|E(H)|} \sum_{\sigma_1,\ldots,\sigma_N=\pm 1} \prod_{i=1}^{N} \sigma_i^{d_H(i)}$$

$$= \sum_{H \text{ subgraph of } G} v^{|E(H)|} \left(\sum_{\sigma_1=\pm 1} \sigma_1^{d_H(1)}\right)\left(\sum_{\sigma_2=\pm 1} \sigma_2^{d_H(2)}\right) \cdots \left(\sum_{\sigma_N=\pm 1} \sigma_N^{d_H(N)}\right),$$

$$(5.10)$$

where $d_H(i)$ denotes the degree of vertex $i$ of $G$ in the subgraph $H$ (in these equations the collection $H$ of edges of $G$ is viewed as a subgraph of $G$ whose vertex set is $V(G)$ and whose edge set is $H$). However, one clearly has

$$\sum_{\sigma=\pm 1} \sigma^d = \begin{cases} 2, & \text{if } d \text{ is even,} \\ 0, & \text{if } d \text{ is odd.} \end{cases} \qquad (5.11)$$

Thus the only non-zero summands in (5.10) are those corresponding to subgraphs $H$ in which all degrees are even; we call such subgraphs *even* subgraphs. Putting (5.9)–(5.11) together we obtain the rewriting of the partition function called high temperature expansion.

LEMMA 5.5 (HIGH TEMPERATURE EXPANSION). *The partition function of the Ising model on any finite graph $G$ can be rewritten as*

$$Z = 2^{|V(G)|} (\cosh(k))^{|E(G)|} \sum_{H \text{ even subgraph of } G} v^{|E(H)|}. \tag{5.12}$$

# Lecture 6

## The Fisher construction and the proofs of Theorems 5.2 and 5.3

Even subgraphs of a given graph $G$ (i.e., subgraphs in which all vertex degrees are even) are also called *polygons* of $G$ (the motivation being that even subgraphs are unions of edge-disjoint cycles; see Lecture 7). An interesting consequence of the high temperature expansion (Lemma 5.5) is that we can determine the number of polygons of any finite graph.

PROPOSITION 6.1. *Let $G$ be a finite connected graph. Then the number of polygons of $G$ is equal to $2^{|E(G)|-|V(G)|+1}$.*

*Proof.* By (5.7) and (5.12) we have

$$\sum_{\{\sigma\}} \prod_{\text{edges}\{i,j\}} e^{k\sigma_i\sigma_j} = 2^{|V(G)|}(\cosh(k))^{|E(G)|} \sum_{H \text{ even subgraph of } G} v^{|E(H)|}. \qquad (6.1)$$

Let $k \to \infty$ in (6.1). As $\cosh(k) = \frac{e^k+e^{-k}}{2}$ and $v = \tanh(k) = \frac{e^k-e^{-k}}{e^k+e^{-k}}$, we have that $\cosh(k) \sim \frac{e^k}{2}$ and $v \to 1$ as $k \to \infty$. Therefore, as $k \to \infty$ the right hand side of (6.1) has the asymptotics

$$\text{RHS of } (6.1) \sim 2^{|V(G)|}\left(\frac{e^k}{2}\right)^{|E(G)|} (\# \text{ polygons of } G). \qquad (6.2)$$

How about the left hand side? Clearly, as $k \to \infty$, each term in the sum on the left hand side of (6.1) grows slower or at most at the same rate as $e^{k|E(G)|}$ (since $\sigma_i\sigma_j = \pm 1$). This maximum growth rate is attained only if all products $\sigma_i\sigma_j$ are equal to 1. Since $G$ is connected, this happens for precisely two states: when all $\sigma_i$'s equal 1, and when all equal $-1$. We thus obtain that as $k \to \infty$ the left hand side of (6.1) has the asymptotics

$$\text{LHS of } (6.1) \sim \prod_{\text{edges}\{i,j\}} e^{k(+1)(+1)} + \prod_{\text{edges}\{i,j\}} e^{k(-1)(-1)} = 2(e^k)^{|E(G)|}. \qquad (6.3)$$

Setting equal the right hand sides of (6.2) and (6.3) and solving for the number of polygons of $G$ we obtain equation (6.1). $\qquad \square$

The proof of Theorem 5.3 will follow from the above proposition when combined with the following classical construction due to Fisher.

PROPOSITION 6.2 (FISHER'S CONSTRUCTION). *Let $G$ be a cubic graph, and let $F = F(G)$, the Fisher graph of $G$, be the graph obtained from $G$ by "inflating" each vertex into a 3-cycle (i.e., for each edge $e$ of $G$, include in $V(F)$ two vertices for the two endpoints of $e$, an edge in $E(F)$ connecting them, and then include an edge in $E(F)$ between any two vertices of $V(F)$ corresponding to coinciding endpoints of edges in $G$; see Figure 6.1).*
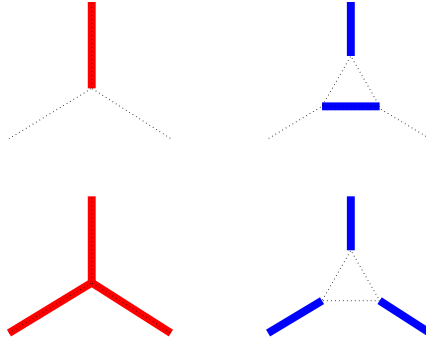
30

Figure 6.1. The possible local configurations in $P^*$ (left)
and the corresponding configurations in $\mu_P$ (right).

*Then there is a bijection between the set of polygons of $G$ and the set of perfect matchings of $F$.*

*Proof.* Given a polygon $P$ of $G$, let $P^*$ be the complement of $P$ in $G$ (i.e., $V(P^*) = V(G)$ and $E(P^*) = E(G) \setminus E(P)$). Since $G$ is cubic and the possible vertex degrees in $P$ are 0 and 2, it follows that all vertex degrees in $P^*$ are either 1 or 3.

Thus, there are only two different ways the neighborhood of a vertex can look in $P^*$; they are shown on the left in Figure 6.1. For each of them, consider the corresponding edge configuration around a 3-cycle in the graph $F$ shown on the right of Figure 6.1. Note that the latter are all compatible, in the sense that if $C$ and $C'$ are neighboring 3-cycles in $F$, then the result of the correspondence in Figure 6.1 around $C$ contains the inter-triangular edge connecting $C$ to $C'$ if and only if the result of the correspondence in Figure 6.1 around $C'$ contains the inter-triangular edge connecting $C$ to $C'$. This, and the fact that on the right of Figure 6.1 each vertex of a 3-cycle is contained in precisely one selected edge, implies that the set of edges resulting by applying this correspondence around each vertex of $P^*$ forms a perfect matching $\mu_P$ of $F$. The map $P \to \mu_P$ is readily invertible. Indeed, given a perfect matching $\mu$ of $F$, contract the 3-cycles to single vertices to obtain a subgraph of $G$ all of whose vertex degrees are 1 or 3; then take the complement of the latter in $G$ to obtain a polygon $P_\mu$ of $G$. It is immediate to check that $P \to \mu_P$ and $\mu \to P_\mu$ are inverses of one another. $\qquad\square$

We can now easily deduce the statement of Theorem 5.3.

*Proof of Theorem 5.3.* Let $G$ be a 3-regular terminal graph, and let $H$ be the graph obtained from $G$ by contracting its triangular cells to single vertices. Then clearly $H$ is cubic and $G$ is the Fisher graph $F(H)$. We then have

$$\mathrm{M}(G) = \mathrm{M}(F(H)) = \# \text{ polygons of } H = 2^{|E(H)|-|V(H)|+1}, \qquad (6.4)$$

where the second equality holds by Proposition 6.2, and the third one by Proposition 6.1.

To see that the right hand side of (6.4) agrees with that of (5.3), note that

$$\sum_{x \in V(H)} \deg(x) = 2|E(H)|,$$

31

and since $H$ is cubic this implies $3|V(H)| = 2|E(H)|$. Furthermore, since $G = F(H)$, it follows that $|V(G)| = 3|V(H)|$. Thus the exponent on the right hand side of (6.4) is $|V(G)|/2 - |V(G)|/3 + 1$, and (5.3) follows. $\qquad\square$

Next, we deduce Theorem 5.2 from Theorem 5.3. To do this, we need one more idea, phrased in the following result.
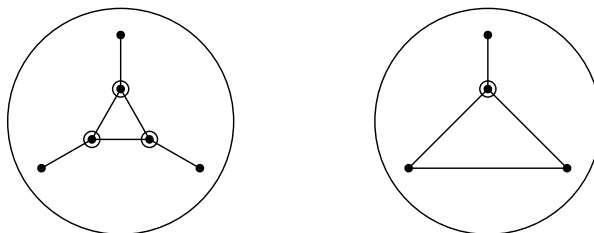


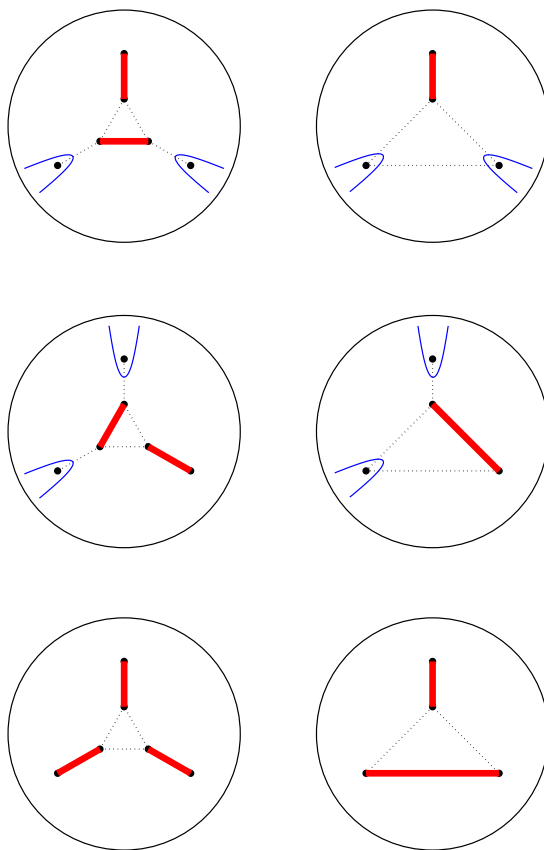Figure 6.2. The circled vertices have no other neighbors besides the ones shown.



Figure 6.3.

LEMMA 6.3 (FUNNY SPIDER LEMMA). *Let $G$ be a graph containing the local configuration shown on the left of Figure 6.2, i.e. a 3-cycle $C$ whose vertices have degree 3, so that the three vertices outside $C$ that have neighbors in $C$ are distinct. Let $G'$ be the graph*

*obtained from $G$ by "cutting out" this local configuration and replacing it with the one on the right of Figure 6.2. Then* $\mathrm{M}(G) = \mathrm{M}(G')$.

*Proof.* Partition the set $\mathcal{M}(G)$ of perfect matchings of $G$ into classes according to which of the three outer vertices in the 3-legged spider on the left of Figure 6.2 are matched to the outside. Since there are 3 internal vertices, the number of outer vertices matched to the outside must be even. We thus obtain a partition of $\mathcal{M}(G)$ into four classes: one corresponding to the top entry in the left column of Figure 6.3, two to the middle entry and its reflection across its vertical symmetry axis, and one to the bottom entry of this column. Partition $\mathcal{M}(G')$ in an analogous way, using the entries of the right column of Figure 6.3. As indicated in Figure 6.3, there is a bijection between corresponding classes of these two partitions. These combine to give a bijection between $\mathcal{M}(G)$ and $\mathcal{M}(G')$. □
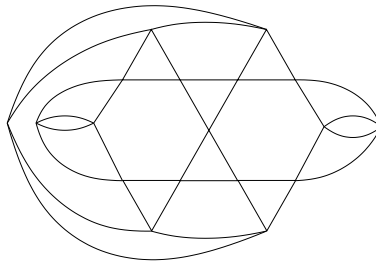


Figure 6.4.
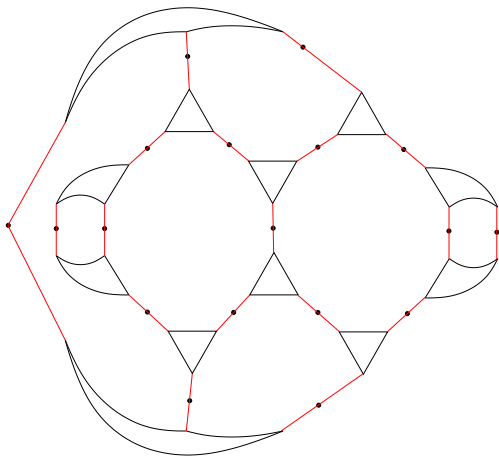


FIGURE 6.5.
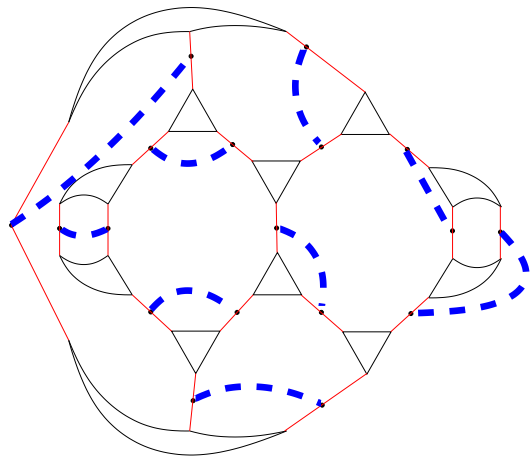


FIGURE 6.6.

*Proof of Theorem 5.2.* Let $G$ be a 4-regular tricellular graph (an example is illustrated in Figure 6.4). Let $G'$ be the graph obtained from $G$ by doing vertex splitting at every vertex, in such a way that same cell neighbors of a vertex remain on the same side after vertex splitting (when $G$ is as shown in Figure 6.4, $G'$ is the graph pictured in Figure 6.5). Note that in $G'$ there are many opportunities to apply the funny spider lemma (Lemma 6.3), and the effect of each application is to replace two paths of length two by two single

33

edges. If one could apply the funny spider lemma in a consistent way so that each path of length two is involved precisely once, the resulting graph $G''$ would be the 3-regular terminal graph obtained from $G$ by stretching out each vertex into an edge connecting two triangular cells, and we could apply Theorem 5.3. Note that this consistent application of Lemma 6.3 is achieved if there exists a way to pair up the paths of length two in $G'$ in disjoint pairs, so that in each pair the paths of length two are incident to a common 3-cycle (such a pairing for our example is indicated in Figure 6.6). But such a pairing is equivalent to a perfect matching of $G$! Since the existence of a perfect matching of $G$ is guaranteed by Lemma 7.4 in the next lecture, the idea mentioned above can be put into practice, and we obtain

$$\mathrm{M}(G) = \mathrm{M}(G') = \mathrm{M}(G''). \tag{6.5}$$

However, by Theorem 5.3 we have

$$\mathrm{M}(G'') = 2^{\frac{|V(G'')|}{6}+1} = 2^{\frac{|V(G)|}{3}+1}, \tag{6.6}$$

as $G''$ has twice as many vertices as $G$. By (6.5) and (6.6) the proof is complete. $\qquad \square$

## Lecture 7

## A different proof of the formula for the number of polygons of a graph

A key point in our proofs of Theorems 5.2 and 5.3 was Proposition 6.1, which states that the number of polygons of any finite graph $G$ is $2^{|E(G)|-|V(G)|+1}$. Given the simple form of the answer, it is surprising that we had to derive this by using the Ising model.

As it turns out, there exists a more direct proof of Proposition 6.1, which we present in this lecture. Let us say right away, however, that merits of the Ising model argument remain. We will show another application of it in the next lecture. For that application, the Ising model argument seems to be the most direct approach.

The alternative proof of Proposition 6.1 mentioned above concerns the cycle space of a graph. The presentation below follows [**9**] (but our proof of Lemma 7.1 is more direct).

Let $G$ be a finite graph, and let $\mathcal{E}(G)$ be the set of subsets of the edge set $E(G)$ of $G$. Endow $\mathcal{E}(G)$ with a vector space structure over the field $\mathbb{F}_2$ with two elements as follows. Given $A, B \subseteq E(G)$ and $\alpha, \beta \in \mathbb{F}_2$, define

$$\alpha A + \beta B \tag{7.1}$$

to consist of those edges $e$ for which $\alpha \chi_e(A) + \beta \chi_e(B) = 1$ in $\mathbb{F}_2$, where $\chi_e(S)$ is 1 if $S$ contains $e$, and 0 otherwise.

Let $\mathcal{C}(G)$ be the subspace of $\mathcal{E}(G)$ spanned by the cycles of $G$.

LEMMA 7.1. *Let $G$ be a connected multigraph. Then $\dim_{\mathbb{F}_2} \mathcal{C}(G) = |E(G)| - |V(G)| + 1$.*

*Proof.* Let $T$ be a spanning tree of $G$ (which exists, as $G$ is connected). $T$ has $|V(G)|-1$ edges. Let $e$ be one of the other $\nu := |E(G)| - |V(G)| + 1$ edges of $G$. The endpoints of $e$ are connected by a unique path $P_e$ in $T$. Define $C_e := P_e \cup e$. Then $C_e$ is a cycle of $G$. Let $e_1, \ldots, e_\nu$ be the edges in $E(G) \setminus E(T)$. Write $C_i$ for $C_{e_i}$. We prove that $\{C_i : i = 1, \ldots, \nu\}$ is a basis of $\mathcal{C}(G)$. This will clearly imply the statement of the lemma.

To check linear independence, assume that $\alpha_1 C_1 + \cdots \alpha_\nu C_\nu = 0$. For any fixed $i$ between 1 and $\nu$, the only cycle containing $e_i$ is $C_i$. Thus the above equality implies $\alpha_i = 0$, which verifies linear independence.

To complete the proof we need to show that any linear combination $L$ of cycles of $G$ is in the span of $\{C_i : i = 1, \ldots, \nu\}$. We prove this by induction on $|L \setminus E(T)|$.

If $|L \setminus E(T)| = 0$, $L$ is a subset of the edges of $T$. We claim that this implies $L = \emptyset$. Indeed, suppose $L \neq \emptyset$. By Lemma 7.2, $L$ viewed as a subgraph of $G$ has all vertex degrees at least 2. But then we can start at some vertex of $L$ and travel along edges so that we leave from each vertex $v$ visited for the first time along an edge different from the edge that led to $v$. This implies the existence of a cycle in $L$, contradicting $L \subseteq E(T)$.

Let $L$ be a linear combination of cycles with $|L \setminus E(T)| > 0$, and let $e \in L \setminus E(T)$. Write

$$L = C_e + (L + C_e). \tag{7.2}$$

Since $L + C_e$ has fewer edges outside $T$ than $L$, it is in the span of $\{C_i : i = 1, \ldots, \nu\}$ by the induction hypothesis. Thus by (7.2) the induction step works, and the proof is complete. $\qquad\square$

LEMMA 7.2. *Let $G$ be a connected multigraph, and identify each polygon on $G$ with its edge set. Regarded this way, the set of polygons on $G$ is precisely $\mathcal{C}(G)$.*

*Proof.* One readily checks that for any polygon $P$ and cycle $C$, $P + C$ is a polygon. Using this it readily follows that the sum of any number of cycles is a polygon (use induction on the number of cycles).

To prove the converse, fix a spanning tree $T$ of $G$, and let $P$ be a polygon on $G$. We prove that $E(P) \in \mathcal{C}(G)$ by induction on $|E(P) \setminus E(T)|$. When $|E(P) \setminus E(T)| = 0$, $P$ is a subgraph of $T$. If $P \neq \emptyset$, the fact that all degrees in $P$ are even implies that $P$ has a cycle. This is then a cycle of the tree $T$, a contradiction showing that we must have $P = \emptyset$ in this case.

Let now $P$ be a polygon with $|E(P) \setminus E(T)| > 0$, and assume that all polygons that have fewer edges outside $T$ than $P$ does are in $\mathcal{C}(G)$. Let $e \in E(P) \setminus E(T)$. The induction step follows by writing $P = C_e + (P + C_e)$ (where $C_e$ is defined as in the proof of Lemma 7.1), and noticing that $P + C_e$ is a polygon with fewer edges outside $T$ than $P$. $\qquad\square$

*Second proof of Proposition 6.1.* By Lemma 7.2, the number of polygons of $G$ equals $|\mathcal{C}(G)|$. However, by Lemma 7.1, each element in the cycle space $\mathcal{C}(G)$ can be written uniquely in the form

$$\alpha_1 C_1 + \cdots \alpha_\nu C_\nu,$$

where $\nu = |E(G)| - |V(G)| + 1$, $C_1, \ldots, C_\nu$ are the cycles defined in the proof of Lemma 7.1, and $\alpha_i \in \{0,1\}$, for $i = 1, \ldots, \nu$. Thus $|\mathcal{C}(G)| = 2^\nu$, and the proof is complete. $\qquad\square$

We present now the result on the existence of a perfect matching that we used in the previous lecture when we proved Theorem 5.2.

In the proof of Lemma 7.4 we will employ the following classical result due to T. Gallai. A 3-edge connected graph is a connected graph that stays connected after the removal of any two of its edges.

THEOREM 7.3 (GALLAI). *Every 3-edge connected 4-regular graph on an even number of vertices has a perfect matching.*

LEMMA 7.4. *Any connected 4-regular tricellular graph with an even number of vertices has a perfect matching.*

*Proof.* The only possible way to disconnect a connected tricellular graph by removing two edges is if the two deleted edges are in the same cell (deleting at most one edge per cell keeps all cells, and thus the graph, connected). Deletion of two edges of the same cell results in disconnecting the graph if and only if their common vertex is a cut-vertex of the graph (i.e., its removal disconnects the graph).

We prove the statement of the lemma by induction on the number of vertices. As $|V(G)|$ is even by hypothesis and since $3t = 2|V(G)|$ (where $t$ is the number of triangular cells of $G$), it follows that $|V(G)|$ is a multiple of 6. Any 4-regular tricellular graph on 6 vertices is isomorphic with the one shown in Figure 7.1, which clearly has a perfect matching.

Let $G$ be a connected 4-regular tricellular graph with an even number of vertices having more than 6 vertices. If $G$ has no cut-vertex, we are done by Theorem 7.3. So let $v$ be
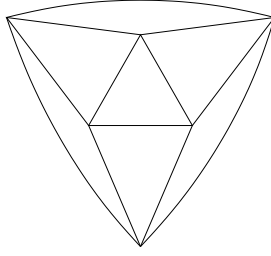
Figure 7.1.

a cut-vertex of $G$: $G \setminus v$ consists of two disconnected parts, which we call $G_l$ and $G_r$ (from left and right; see Figure 7.2). Without loss of generality we may assume that the number of vertices of $G_l$ is even, and that of $G_r$ is odd.
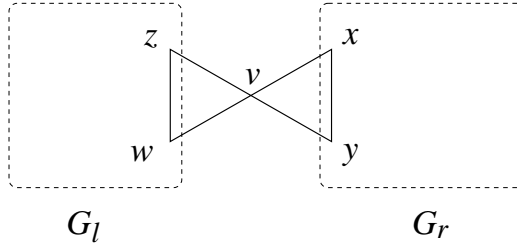


Figure 7.2.

Let $\tilde{G}_r$ be the graph obtained from $G_r \setminus xy$ by identifying vertices $x$ and $y$, the neighbors of $v$ that belong to $G_r$. Then $\tilde{G}_r$ has a perfect matching $\mu_r$ by the induction hypothesis.

Define $\tilde{G}_l$ to be the graph obtained from $G_l \setminus zw$ by adjoining two new vertices $a$ and $b$ which form two new triangular cells together with the neighbors $z$ and $w$ of $v$ that belong to $G_l$ (see Figure 7.3). Then $\tilde{G}_l$ has a perfect matching $\mu_l$ by the induction hypothesis (it has fewer vertices than $G$, as $G$ has at least three vertices outside $G_l$, namely $v$, $x$, and $y$).
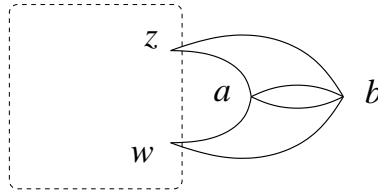


Figure 7.3. The graph $\tilde{G}_l$.

Since $\mu_l$ is a perfect matching, one of the following is necessarily true: $(i)$ one of the $ab$ edges is in $\mu_l$; $(ii)$ $aw, bz \in \mu_l$; or $(iii)$ $az, bw \in \mu_l$. In case $(i)$, $\mu_l \setminus ab$ is a perfect matching of $G_l$. In case $(ii)$, $(\mu_l \setminus \{aw, bz\}) \cup zw$ is a perfect matching of $G_l$; case $(iii)$ is equivalent to case $(ii)$. Thus $\mu_l$ generates a perfect matching $\mu_l'$ of $G_l$.

Depending on whether the vertex of $\tilde{G}_r$ obtained by identifying $x$ and $y$ is matched by $\mu_r$ to a former neighbor of $x$ or to a former neighbor of $y$, $\tilde{G}_r$ generates a perfect

matching $\mu'_r$ of $G_r \setminus y$ or $G_r \setminus x$, respectively. Then $\mu'_l \cup \mu'_r \cup vy$ (resp., $\mu'_l \cup \mu'_r \cup vx$ is a perfect matching of $G$. This completes the proof. $\qquad\square$

# Lecture 8

## Dimer coverings of 4-regular tricellular graphs
## with exactly two monomers: Part I

So far we have looked at the situation when disjoint edges ("dimers") cover completely the vertex set of a graph. It is interesting to change this point of view and consider the situation when the dimer covering is not quite complete, but leaves uncovered say precisely two vertices ("monomers").

This question was first considered by Fisher and Stephenson in the early 1960's, in the context of square grid graphs. Figure 8.1 shows a dimer covering of the $4 \times 4$ grid graph which leaves two vertices uncovered.
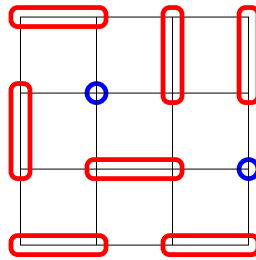


Figure 8.1. Two monomers in a sea of dimers.

Natural questions one can ask include:

($i$) If we fix two vertices $a$ and $b$ of a graph $G$, how does $\mathrm{M}(G \setminus \{a, b\})$ relate to $\mathrm{M}(G)$?

($ii$) How does $\mathrm{M}(G \setminus \{a, b\})$ vary as $a$ and $b$ run over $V(G)$?

For large subgraphs $G$ of $\mathbb{Z}^2$, the answer to ($ii$) above turns out to be given by a close parallel to two dimensional electrostatics. Namely, if $a$ and $b$ have opposite colors in the chessboard coloring of $\mathbb{Z}^2$, then in the limit as $G$ grows infinitely large, while $a$ and $b$ stay relatively close to its "center," $\mathrm{M}(G \setminus \{a, b\})$ decays proportionally to $\mathrm{d}(a, b)^{-1/2}$, while if $a$ and $b$ have the same color, then $\mathrm{M}(G \setminus \{a, b\})$ grows proportionally to $\mathrm{d}(a, b)^{1/2}$, as $\mathrm{d}(a, b) \to \infty$ (here d denotes the Euclidean distance); note that if one assigns charge $+1$ to the white vertices and charge $-1$ to the black ones, the exponents above equal $1/2$ times the product of the charges of the missing vertices. Details about this are presented in [4], [6], [7], and [8].

In the case of 4-regular tricellular graphs, the situation turns out to be completely different. As we will see in this lecture and the next, $\mathrm{M}(G \setminus \{a, b\})$ turns out to be *constant* in this case as $a$ and $b$ run over $V(G)$. More precisely, we have the following result.

THEOREM 8.1. *Let $K$ be a 4-regular tricellular graph, and let $a$ and $b$ be two vertices of $K$ that are not neighbors. Let $H$ be the cell graph of $K$: The vertices of $H$ are the cells of $K$, and two such cells are connected by an edge in $H$ whenever they share a common*

*vertex in $G$ (in case two cells of $G$ share $k > 1$ vertices, the corresponding vertices of $H$ are connected by $k$ parallel edges). Let $e_a$ and $e_b$ be the edges of $H$ corresponding to $a$ and $b$, respectively. Assume that $K \setminus \{a, b\}$ has a perfect matching, and that $H$ has a perfect matching containing $e_a$ and $e_b$. Then*

$$\mathrm{M}(K \setminus \{a, b\}) = \frac{1}{4} \, \mathrm{M}(K). \tag{8.1}$$

It turns out that it is possible to modify both Fisher's construction and the high temperature expansion of the Ising model in a way that will allow us to deduce (8.1) in a way analogous to our first proof of Theorem 5.2. In addition we will also need the following modified version of the funny spider lemma (Lemma 6.3).
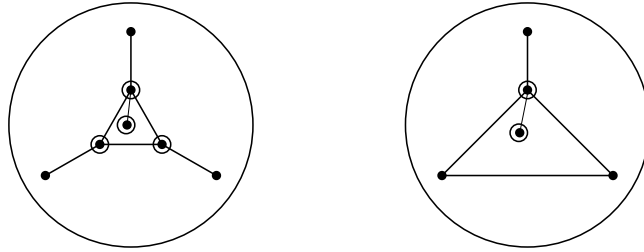


Figure 8.2. The circled vertices have no other neighbors besides the ones shown.

LEMMA 8.2 (MODIFIED FUNNY SPIDER LEMMA). *Let $G$ be a graph containing the local configuration shown on the left of Figure 8.2, i.e. a 3-cycle $C$ whose vertices have degree 3, so that the three vertices outside $C$ that have neighbors in $C$ are distinct, plus a vertex of degree 1 inside $C$ connected to a vertex of $C$. Let $G'$ be the graph obtained from $G$ by "cutting out" this local configuration and replacing it with the one on the right of Figure 8.2. Then $\mathrm{M}(G) = \mathrm{M}(G')$.*

*Proof.* As in the proof of Lemma 6.3, partition the set $\mathcal{M}(G)$ of perfect matchings of $G$ into classes according to which of the three outer vertices in the local pattern on the left of Figure 8.2 are matched to the outside. Since there are now 4 internal vertices, the number of outer vertices matched to the outside must be odd. We thus obtain a partition of $\mathcal{M}(G)$ into four classes: one corresponding to the top entry in the left column of Figure 8.3, two to the middle entry and its reflection across its vertical symmetry axis, and one to the bottom entry of this column. The latter class is actually empty, as it follows from the bottom left picture in Figure 8.3 (the thick edge is forced, and then the central vertex cannot be matched). Partition $\mathcal{M}(G')$ in an analogous way, using the entries of the right column of Figure 8.3. As indicated in Figure 8.3, there is a bijection between corresponding classes of these two partitions. These combine to give a bijection between $\mathcal{M}(G)$ and $\mathcal{M}(G')$. $\qquad\square$

We present next the modified version of the Fisher construction that we will need for our proof of Theorem 8.1.
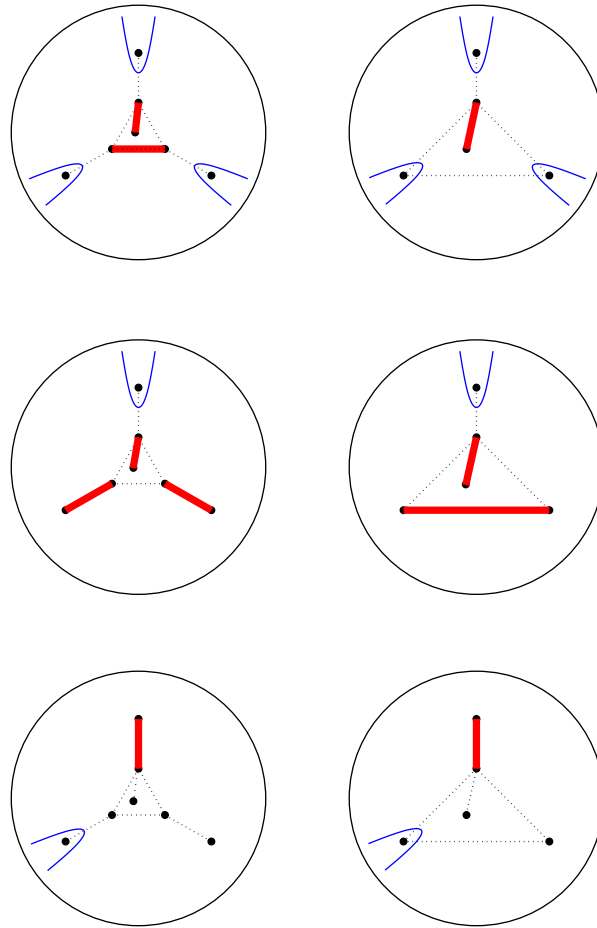
Figure 8.3.
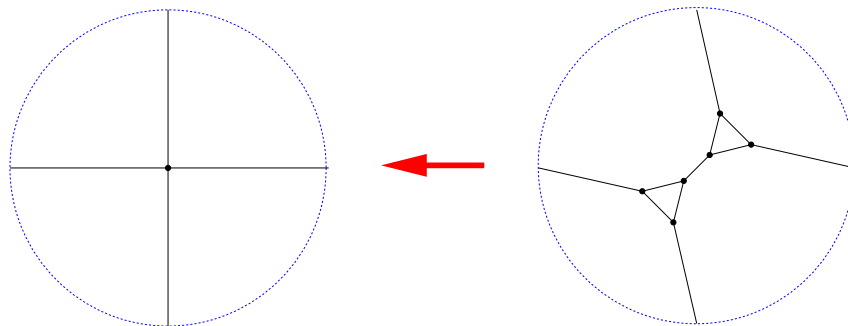


Figure 8.4.

For a 4-regular graph $G$, define its Fisher graph $F(G)$ by replacing each vertex by a "city" of six vertices, as indicated in Figure 8.4. We refer to the two central vertices in each city as the *inner vertices* of that city.

Given two vertices $a$ and $b$ of $G$, we say that a collection $P$ of edges of $G$ forms an $a$, $b$ *near polygon of $G$* if $a$ and $b$ are incident to an odd number of edges of $P$, and every

41

other vertex of $G$ is incident to an even number of edges of $P$.

For a graph with an even number of vertices, a *near perfect matchings* is a collection of disjoint edges that leaves precisely two vertices uncovered.

LEMMA 8.3 (MODIFIED FISHER CONSTRUCTION). *Let $G$ be a 4-regular graph, and let $a$ and $b$ be two of its vertices. Then if $F(G)$ is the Fisher graph of $G$ defined above, there is a bijection between the set of $a$, $b$ near polygons of $G$ and the set of near perfect matchings of $F(G)$ in which precisely one inner vertex in each of the cities corresponding to $a$ and $b$ is left uncovered.*
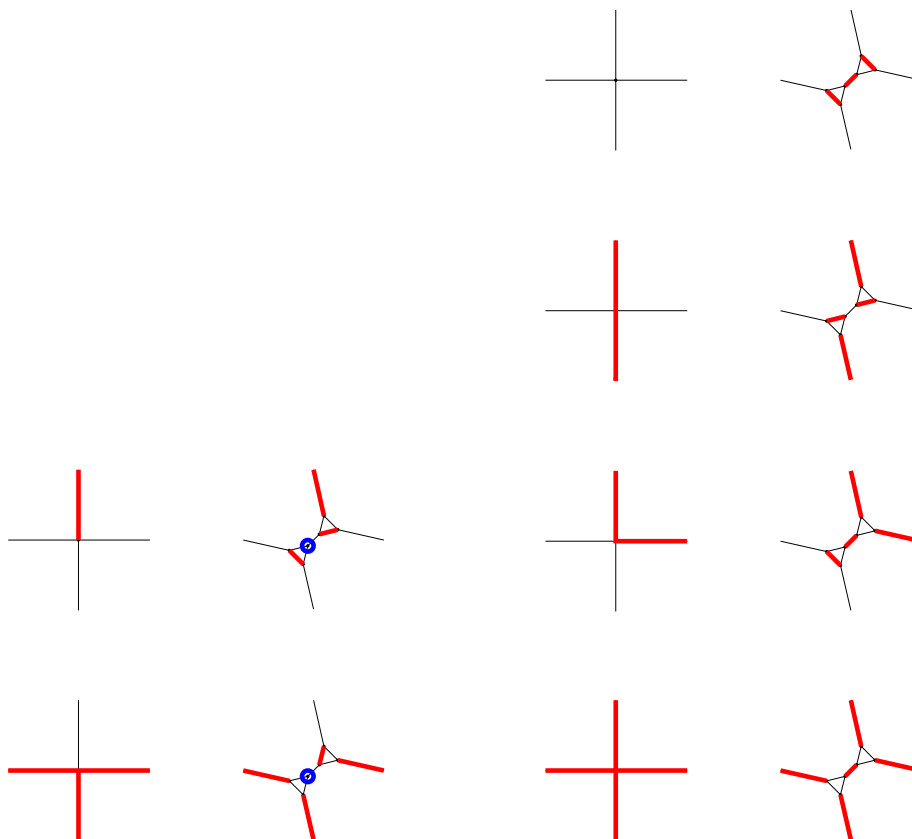


FIGURE 8.5(a)  FIGURE 8.5(b)

*Proof.* The left column of Figure 8.5(a) shows the possible ways (up to rotations by multiples of 90°) of choosing an odd number of edges around a vertex of degree 4. The left column of Figure 8.5(b) shows the possible ways of choosing an *even* number of edges around a vertex of degree 4.

Note that in the Fisher graph $F(G)$ of $G$ there are two types of edges: edges that correspond to the edges of $G$ (which have endpoints in different cities), and edges that connect vertices in the same city; call the former inter-city edges, and the latter inner edges.

Let $P$ be an $a$, $b$ near polygon of $G$, and let $\mu_1$ be the set of inter-city edges of the Fisher graph $F(G)$ that correspond to the edges of $P$. Define the set $\mu_2$ of inner edges of $F(G)$ as follows. For each city $c$ of $F(G)$, consider the edges of $\mu_1$ incident to $c$, look up the corresponding pattern in the right columns of Figures 8.5(a) and (b), and include in $\mu_2$ the inner edges of $c$ that this pattern specifies. Note that all vertices shown in the right column of Figure 8.5(b) are incident to precisely one thick edge, and, with the exception of a single inner vertex (which is not incident to any thick edge), the same is true for the vertices shown in the right column of Figure 8.5(a) (in addition, one readily checks that the displayed choices of inner edges are the unique choices with these properties). It follows that $\mu_P := \mu_1 \cup \mu_2$ is an $a$, $b$ near perfect matching of $F(G)$.

Conversely, if $\mu$ is a near perfect matching of $F(G)$ which leaves precisely one inner monomer uncovered in each of the cities corresponding to $a$ and $b$, then clearly $\mu$ contains an odd number of inter-city edges incident to each of the cities corresponding to $a$ and $b$, and an even number of inter-city edges incident to any other city. Thus the set of edges of $G$ corresponding to the inter-city edges of $\mu$ forms an $a$, $b$ near polygon $P_\mu$.

It follows by construction that $P_{\mu_P} = P$. The equality $\mu_{P_\mu} = \mu$ follows from the uniqueness of the choices of the inner edges in the right columns of Figures 8.5(a) and (b) mentioned towards the end of the third paragraph of this proof. $\qquad\square$

# Lecture 9

## Dimer coverings of 4-regular tricellular graphs
## with exactly two monomers: Part II

We need one more fact before giving the proof of Theorem 8.1. It is an analog of Proposition 6.1.

PROPOSITION 9.1. *Let $G$ be a finite connected graph, and let $a$ and $b$ be two vertices of $G$. Then the number of $a$, $b$ near polygons of $G$ is equal to $2^{|E(G)|-|V(G)|+1}$.*

*Proof.* Consider the Ising model on $G$, and let $Z_{a,b}$ be defined by

$$Z_{a,b} := \sum_{\{\sigma\}} \sigma_a \sigma_b \prod_{\text{edges}\{i,j\}} e^{k\sigma_i\sigma_j} \tag{9.1}$$

(note that this is obtained from the partition function (5.7) by sticking in the prefactor $\sigma_a\sigma_b$ in front of the summand). The very same arguments that proved (5.10) give

$$Z_{a,b} =$$

$$\sum_{H \text{ subgraph of } G}$$

$$\left\{ v^{|E(H)|} \left( \sum_{\sigma_1=\pm1} \sigma_1^{d_H(1)} \right) \cdots \left( \sum_{\sigma_{a-1}=\pm1} \sigma_{a-1}^{d_H(a-1)} \right) \left( \sum_{\sigma_a=\pm1} \sigma_a^{d_H(a)+1} \right) \left( \sum_{\sigma_{a+1}=\pm1} \sigma_{a+1}^{d_H(a+1)} \right) \right.$$

$$\left. \cdots \left( \sum_{\sigma_{b-1}=\pm1} \sigma_{b-1}^{d_H(b-1)} \right) \left( \sum_{\sigma_b=\pm1} \sigma_b^{d_H(b)+1} \right) \left( \sum_{\sigma_{b+1}=\pm1} \sigma_{b+1}^{d_H(b+1)} \right) \cdots \left( \sum_{\sigma_N=\pm1} \sigma_N^{d_H(N)} \right) \right\}.$$

$$\tag{9.2}$$

Using now (5.11) it follows that

$$Z_{a,b} = 2^{|V(G)|}(\cosh(k))^{|E(G)|} \sum_{H \ a, \ b \text{ near polygon of } G} v^{|E(H)|}. \tag{9.3}$$

As in the proof of Proposition 6.1, let $k \to \infty$ on both sides of equation (9.3). The asymptotics of the right hand side is given by the expression in (6.2), with the number of polygons replaced by the number of $a$, $b$ near polygons. The dominant terms as $k \to \infty$ on the left hand side of (9.3) are those terms in the sum (9.2) for which all exponents are 1 and $\sigma_a\sigma_b = 1$. This happens for precisely two states, the all 1 and all $-1$ states; their contribution is the same as in (6.3). Setting equal the $k \to \infty$ asymptotics of the two sides of (9.3) and solving for the number of $a$, $b$ near polygons completes the proof. $\quad\square$

44

*Proof of Theorem 8.1.* Let $K$ be a 4-regular tricellular graph with the properties in the hypotheses of Theorem 8.1 (an illustrative example is shown in Figure 9.1). Let $K_{a,b}$ be the graph obtained from $K$ by adding two new vertices $a'$ and $b'$, with $a'$ adjacent only to $a$ and $b'$ only to $b$. Then we clearly have

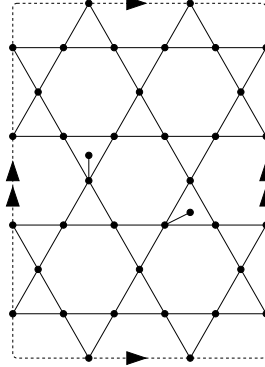$$\mathrm{M}(K \setminus \{a, b\}) = \mathrm{M}(K_{a,b}). \tag{9.4}$$



Figure 9.1. An illustrative example of the graph $K_{a,b}$.

Let $K_{a,b}^{\mathrm{up,up}}$ be the graph obtained from $K_{a,b}$ by drawing the new edge $aa'$ (resp., $bb'$) inside the upper of the two cells containing $a$ (resp., $b$), and then doing vertex splitting at each original vertex; for the graph shown in Figure 9.1, $K_{a,b}^{\mathrm{up,up}}$ is illustrated in Figure 9.2. Three other graphs, $K_{a,b}^{\mathrm{up,down}}$, $K_{a,b}^{\mathrm{down,up}}$ and $K_{a,b}^{\mathrm{down,down}}$, can be defined analogously.

By the vertex splitting lemma (Lemma 2.2) we have

$$\mathrm{M}(K_{a,b}) = \mathrm{M}(K_{a,b}^{\mathrm{up,up}}). \tag{9.5}$$

Note that around the 3-cycles of $K_{a,b}^{\mathrm{up,up}}$ there are several different opportunities to apply the funny spider lemma (Lemma 6.3) or the modified funny spider lemma (Lemma 8.2). The effect of each of these is to replace two paths of length 2 incident to that 3-cycle by paths of length 1. We claim that it is possible to choose a way to apply one of these two lemmas around every 3-cycle of $K_{a,b}^{\mathrm{up,up}}$ in such a way that all paths of length 2 connecting different 3-cycles (from here on referred to simply as 2-paths) are converted into paths of length 1 (i.e., single edges); for the illustrated example, one such way of applying the two lemmas is indicated in Figure 9.3.

Indeed, if a 3-cycle $C$ doesn't contain any of the two new edges, Lemma 6.3 can be applied in three different ways around $C$ — each such way being determined by a pair of 2-paths incident to $C$. On the other hand, if $C$ contains a new edge, Lemma 8.2 can be applied in only one way around $C$, determined by pairing up the 2-paths not incident to the new edge. Thus, to achieve what we claimed, we need a perfect matching of the graph whose vertices are the 2-paths of $K_{a,b}^{\mathrm{up,up}}$, with two such vertices connected by an edge iff the corresponding 2-paths are incident to the same 3-cycle (except around the 3-cycles
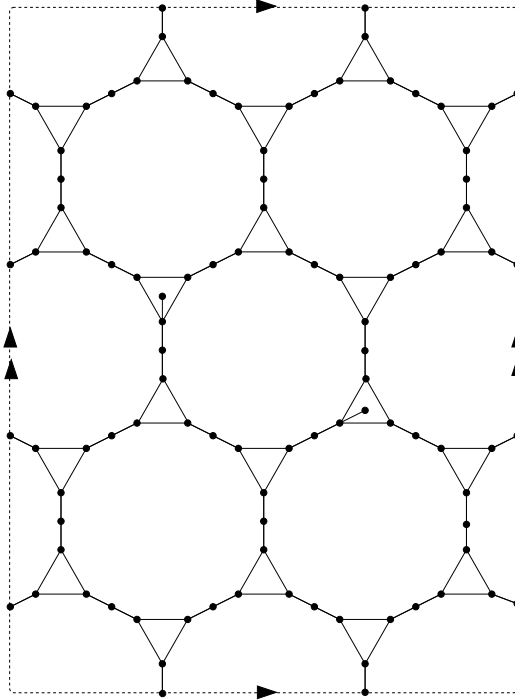
45

Figure 9.2. The graph $K_{a,b}^{\mathrm{up,up}}$ for the example in Figure 9.1.
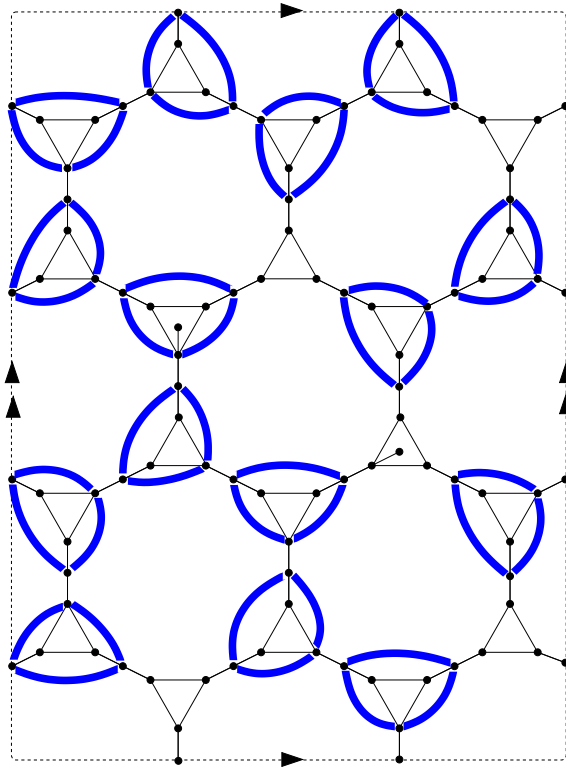


Figure 9.3. Applying the funny spider lemma and the modified funny spider lemma.

46

containing a new edge, where only the two 2-paths not incident to any of the new edges are connected by an edge). However, the graph just described is isomorphic to the graph obtained from $K$ by deleting two of the edges incident to $a$ and two of those incident to $b$! The existence of a perfect matching of the latter follows from our assumption that $K \setminus \{a, b\}$ has a perfect matching. This proves our claim. Denoting by $\tilde{K}_{a,b}^{\mathrm{up,up}}$ the graph obtained from $K_{a,b}^{\mathrm{up,up}}$ by replacing all 2-paths by single edges, we obtain

$$\mathrm{M}(K_{a,b}^{\mathrm{up,up}}) = \mathrm{M}(\tilde{K}_{a,b}^{\mathrm{up,up}}). \tag{9.6}$$

Let $\tilde{K}_{a,b}^{\mathrm{up,down}}$, $\tilde{K}_{a,b}^{\mathrm{down,up}}$ and $\tilde{K}_{a,b}^{\mathrm{down,down}}$ be the graphs obtained by the same procedure for the other choices for drawing the two new edges inside cells of $K$. Clearly (9.6) holds with any of them on the right hand side. Thus, by (9.4) and (9.5)–(9.6) and their analogs we obtain

$$4\,\mathrm{M}(K \setminus \{a, b\}) = \mathrm{M}(\tilde{K}_{a,b}^{\mathrm{up,up}}) + \mathrm{M}(\tilde{K}_{a,b}^{\mathrm{up,down}}) + \mathrm{M}(\tilde{K}_{a,b}^{\mathrm{down,up}}) + \mathrm{M}(\tilde{K}_{a,b}^{\mathrm{down,down}}). \tag{9.7}$$

Denote by $\tilde{K}$ the graph obtained from $K$ by separating its cells so they become vertex disjoint, and including new edges between vertices that used to coincide in $K$. Denote by $f_a$ and $f_b$ the new edges of $\tilde{K}$ corresponding to $a$ and $b$, respectively. By definition, we have

$$\mathrm{M}(\tilde{K}_{a,b}^{\mathrm{up,up}}) + \mathrm{M}(\tilde{K}_{a,b}^{\mathrm{up,down}}) + \mathrm{M}(\tilde{K}_{a,b}^{\mathrm{down,up}}) + \mathrm{M}(\tilde{K}_{a,b}^{\mathrm{down,down}})$$

$$= \# \ \{\text{near perfect matchings of } \tilde{K} \text{ in which precisely one endpoint}$$

$$\text{of each of } e_a \text{ and } e_b \text{ is left uncovered}\} \tag{9.8}$$

(see also Figure 9.4).

We use now the hypothesis that the cell graph $H$ of $K$ has a perfect matching containing the two edges $e_a$ and $e_b$. It implies that the 3-cycles of $\tilde{K}$ can be grouped into disjoint pairs of neighbors so that the two 3-cycles bordering $f_a$ are paired together, and the two 3-cycles bordering $f_b$ are paired together. But two neighboring 3-cycles form a pattern isomorphic to a city in a Fisher graph of a 4-regular graph (one choice for this pairing in the case of our illustrative example is shown in Figure 9.5). Denoting by $\bar{K}$ the graph obtained from $\tilde{K}$ by contracting all such cities to single vertices, we obtain by (9.7), (9.8) and the modified Fisher construction of Lemma 8.3 that

$$4\,\mathrm{M}(K \setminus \{a, b\}) = \#\ a, b \text{ near polygons of } \bar{K}. \tag{9.9}$$

By Proposition 9.1, the right hand side of (9.9) is $2^{|E(\bar{K})| - |V(\bar{K})| + 1}$. Since 6-vertex cities in $\tilde{K}$ are contracted to single vertices in the definition of $\bar{K}$, we have $|V(\tilde{K})| = 6|V(\bar{K})|$. We also clearly have $|V(\tilde{K})| = 2|V(K)|$, implying $|V(\bar{K})| = \frac{1}{3}|V(K)|$. As $\bar{K}$ is 4-regular, it follows that $4|V(\bar{K})| = 2|E(\bar{K})|$, hence $|E(\bar{K})| = 2|V(\bar{K})| = \frac{2}{3}|V(K)|$. Therefore the right hand side of (9.9) equals $2^{\frac{|V(K)|}{3} + 1}$, and (8.1) follows by Theorem 5.2. $\qquad \square$
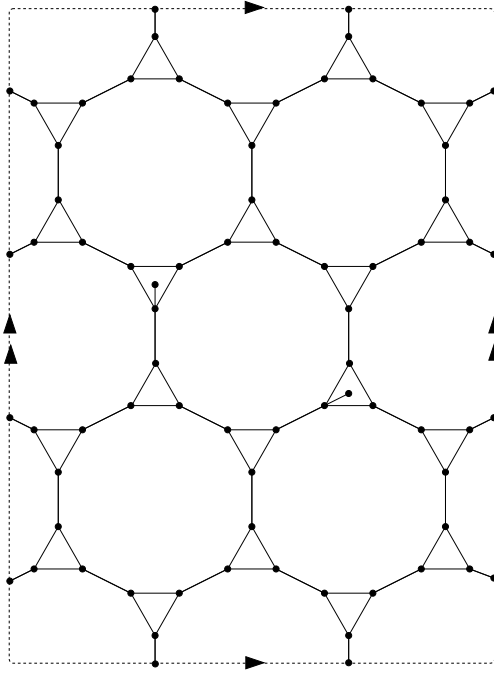
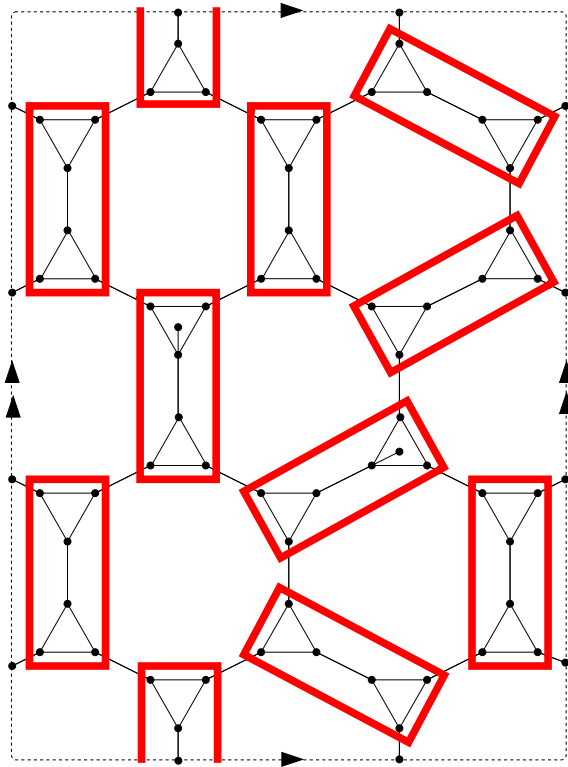Figure 9.4. The graph $\tilde{K}_{a,b}^{\mathrm{up,up}}$.



Figure 9.5. Pairing the 3-cycles of $\tilde{K}_{a,b}^{\mathrm{up,up}}$ into Fisher cities.

# Lecture 10

## A factorization theorem for perfect matchings

In this lecture we justify the trick (1.1) we used in the first lecture to get the number of perfect matchings of some special graphs in a quicker way. Equation (1.1) is a particular case of a more general result which we present below.

Let $G$ be a plane graph. We say that $G$ is *symmetric* if it is invariant under the reflection across some straight line. Figure 10.1 shows an example of a symmetric graph. Clearly, a symmetric graph has no perfect matching unless the axis of symmetry contains an even number of vertices (otherwise, the total number of vertices is odd); we will assume this throughout this lecture.

A *weighted* symmetric graph is a symmetric graph equipped with a weight function on the edges that is constant on the orbits of the reflection. The *width* of a symmetric graph $G$, denoted $w(G)$, is defined to be half the number of vertices of $G$ lying on the symmetry axis.
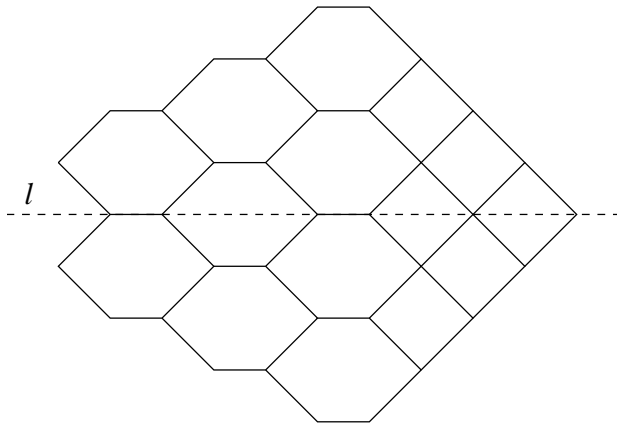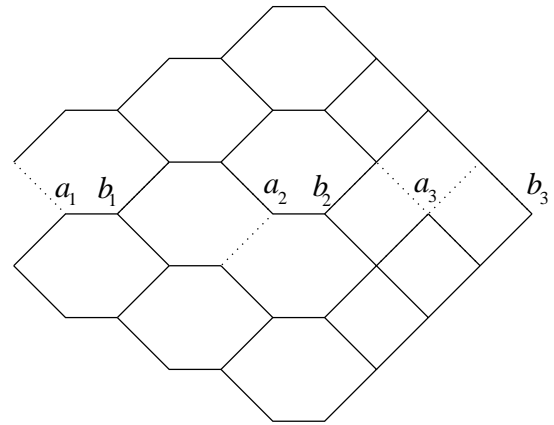


FIGURE 10.1                    FIGURE 10.2

Let $G$ be a weighted symmetric graph with symmetry axis $\ell$, which we consider to be horizontal. Let $a_1, b_1, a_2, b_2, \ldots, a_{w(G)}, b_{w(G)}$ be the vertices lying on $\ell$, as they occur from left to right. Let us call a *reduced* subgraph of $G$ a graph obtained from $G$ by deleting at each vertex $a_i$ either all incident edges above $\ell$ (we refer to this operation for short as "cutting above $a_i$") or all incident edges below $\ell$ ("cutting below $\ell$," for short). Figure 10.2 shows a reduced subgraph of the graph presented in Figure 10.1 (the deleted edges of the original graph are represented by dotted lines).

Recall that the weight of a perfect matching $\mu$ is defined to be the product of the weights of the edges contained in $\mu$. The matching generating function of a weighted graph $G$, denoted $M(G)$, is the sum of the weights of all perfect matchings of $G$. The matching generating function is clearly multiplicative with respect to disjoint unions

of graphs. Therefore there is no loss of generality in assuming that the graphs under consideration are connected.

LEMMA 10.1. *All $2^{\mathrm{w}(G)}$ reduced subgraphs of a weighted symmetric graph $G$ have the same matching generating function.*

*Proof.* It is enough to prove the statement of the lemma for two reduced subgraphs that differ only around a single vertex $a_i$. Let $G_1$ and $G_2$ be two reduced subgraphs obtained by identical cutting operations except that for the former we made a cut above $a_i$, while for the latter we cut below $a_i$ (for some $i \in \{1, 2, \ldots, \mathrm{w}(G)\}$). Let $\mu$ be a perfect matching of $G_1$ and let $\mu'$ be the perfect matching of $G$ obtained from $\mu$ by reflection across $\ell$. Then $\nu = \mu \cup \mu'$ (where the union is a multi-set union) is a 2-factor of $G$ (i.e., each vertex of $G$ is incident to precisely two edges of $\nu$) that is symmetric about $\ell$. Therefore, $\nu$ is a disjoint union of even-length cycles. Consider the cycle $C$ containing $a_i$, and let $C'$ be the reflection of $C$ across $\ell$. Since $\nu$ is symmetric about $\ell$, $C'$ is a cycle of $\nu$. Note that $C' \neq C$ would imply that $C$ is disjoint from $C'$, contradicting $a_i \in C \cap C'$. Therefore $C'$ coincides with $C$, and $C$ is symmetric with respect to $\ell$. Thus, since all vertices of $C$ have degree two, $C$ has only one vertex on $\ell$ besides $a_i$. We claim that this vertex is one of $b_1, b_2, \ldots, b_{\mathrm{w}(G)}$.

Indeed, it follows otherwise that the set of vertices encircled by $C$ has an odd number of elements on $\ell$. Since this set is symmetric about $\ell$, it follows that it has an odd number of elements, contradicting the fact that the 2-factor $\nu$ is a disjoint union of even-length cycles.

Define $\mu''$ to be the perfect matching of $G$ obtained from $\mu$ by replacing $\mu \cap C$ by $\mu' \cap C$. Then clearly $\mu''$ is a perfect matching of $G_2$ and the correspondence $\mu \mapsto \mu''$ is a weight-preserving bijection between the perfect matchings of $G_1$ and those of $G_2$. $\qquad\square$

Let $G$ be a weighted symmetric graph that is also bipartite (i.e., its vertices can be colored black or white so that every edge has a white and a black endpoint). Suppose that the set of vertices lying on $\ell$ is a cut set (i.e., removing these vertices disconnects the graph). In such a case we say that $\ell$ *separates* $G$. Let us color the vertices in the two bipartition classes black and white. For definiteness, choose the leftmost vertex on the symmetry axis $\ell$ to be white. We define two subgraphs $G^+$ and $G^-$ as follows. Perform cutting operations above all white $a_i$'s and black $b_i$'s and below all black $a_i$'s and white $b_i$'s. Note that this procedure yields cuts of the same kind at the endpoints of each edge lying on $\ell$. Reduce the weight of each such edge by half; leave all other weights unchanged. Since $\ell$ separates $G$, the graph produced by the above procedure is disconnected into one component lying above $\ell$, which we denote by $G^+$, and one below $\ell$, denoted by $G^-$. Figure 10.3 illustrates this procedure for the graph pictured in Figure 10.1 (the edges whose weight has been reduced by half are marked by 1/2).

THEOREM 10.2 (FACTORIZATION THEOREM). *Let $G$ be a planar bipartite weighted symmetric graph separated by its symmetry axis. Then*

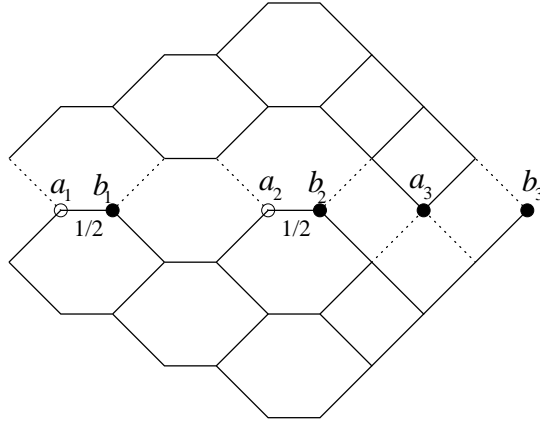$$\mathrm{M}(G) = 2^{\mathrm{w}(G)} \,\mathrm{M}(G^+)\,\mathrm{M}(G^-).$$

FIGURE 10.3

*Proof.* First, we show that we can reduce to the case when there are no edges between any of the vertices of $G$ lying on $\ell$. To see this, we construct a new graph $\tilde{G}$ as follows. Cut the graph $G$ along $\ell$ so that we obtain two copies of each vertex lying on $\ell$, and two copies of each edge contained in $\ell$. Assign half the weight of the original edge to each copy; keep the original weights for all other edges. Finally, insert a new vertex between the two copies of each vertex formerly on $\ell$, and join it to both copies by an edge weighted 1. It is clear that we can carry out this construction such that the resulting graph is symmetric (this is illustrated in Figure 10.4 in the case of the graph $G$ shown in Figure 10.1). Denote it by $\tilde{G}$, and let $\tilde{\ell}$ be its symmetry axis. We claim that $G$ and $\tilde{G}$ have the same matching generating function.
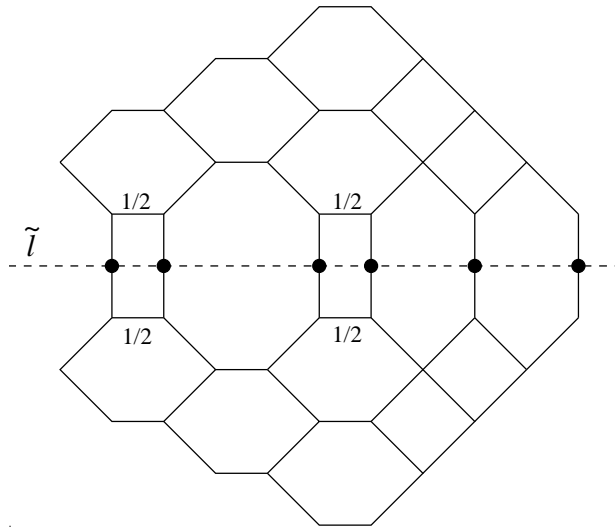


FIGURE 10.4

Indeed, apply in reverse the weighted vertex splitting lemma (Lemma 2.4) to $\tilde{G}$ around each vertex on $\tilde{\ell}$. Wherever there was an edge $e$ of $G$ along $\ell$, two parallel edges of half

51

the weight of $e$ are produced by this process. These are clearly equivalent to a single edge weighted by the weight of $e$, and we obtain $\mathrm{M}(\tilde{G}) = \mathrm{M}(G)$.
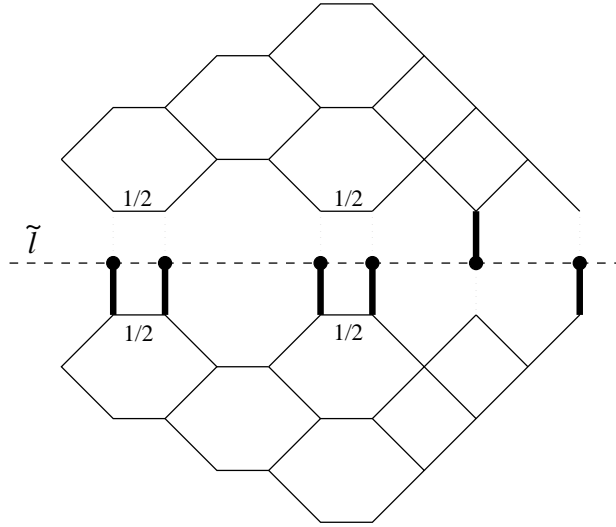


FIGURE 10.5

Note that each vertex of $\tilde{G}^+$ lying on $\tilde{\ell}$ has degree 1, hence any perfect matching of $\tilde{G}^+$ must contain the edge incident to this vertex (see Figure 10.5). Also, by construction, all edges of $\tilde{G}^+$ incident to such vertices have weight equal to 1. Therefore, $\mathrm{M}(\tilde{G}^+)$ is equal to the matching generating function of the subgraph of $\tilde{G}^+$ obtained by deleting the vertices matched by the forced edges of weight 1. However, this subgraph is isomorphic to $G^-$, and we obtain that $\mathrm{M}(\tilde{G}^+) = \mathrm{M}(G^-)$. Similarly, we deduce that $\mathrm{M}(\tilde{G}^-) = \mathrm{M}(G^+)$.

Thus, it is enough to prove the statement of the theorem for a graph $G$ whose vertices lying on $\ell$ don't have any edge between them. According to Lemma 10.1, it is enough to show that $\mathrm{M}(G^+)\,\mathrm{M}(G^-)$ is the matching generating function of some (hence any) of the $2^{\mathrm{w}(G)}$ reduced subgraphs of $G$. We prove this for the reduced graph $H$ obtained by cutting above the white $a_i$'s and below the black $a_i$'s. For this, it suffices to show that every perfect matching of $H$ is also a perfect matching of $G^+ \cup G^-$, i.e., that in every perfect matching $\mu$ of $H$ the white $b_i$'s are matched upward and the black $b_i$'s downward. Let $x$ and $y$ be the number of white and black vertices of $G$ lying above $\ell$, respectively. Let $x_1$ and $y_1$ (resp., $x_2$ and $y_2$) be the number of white and black $a_i$'s (resp., $b_i$'s). We then clearly have

$$2x + x_1 + x_2 = 2y + y_1 + y_2 \tag{10.1}$$

(as the number of white vertices in $G$ must equal the number of black vertices in $G$ in order for $G$ to have any perfect matchings) and

$$x_1 + y_1 = \mathrm{w}(G) = x_2 + y_2. \tag{10.2}$$

Let $\alpha$ and $\beta$ be the number of white and black $b_i$'s matched upward in $\mu$, respectively. We need to show that $\alpha = x_2$ and $\beta = 0$.

Consider the set of edges of $\mu$ that lie above $\ell$. Among their endpoints, $x + \alpha$ are white and $y + y_1 + \beta$ are black, so $x + \alpha = y + y_1 + \beta$. We therefore obtain

$$x_2 \geq \alpha \geq \alpha - \beta = y - x + y_1. \tag{10.3}$$

However, by relations (10.2) and (10.1) we have

$$x_2 - y_1 = \frac{1}{2}((x_2 - y_1) + (x_1 - y_2)) = \frac{1}{2}(2y - 2x) = y - x,$$

so we actually have equality in (10.3). This implies $\alpha = x_2$ and $\beta = 0$, as desired. $\qquad \square$

## Lecture 11

## Temperley's trick and an application

In this lecture we present a very useful connection between perfect matchings and spanning trees. It holds for any planar graphs, but it will be enough for us to present the special case of subgraphs of the grid graph $\mathbb{Z}^2$.

Let $G$ be a finite connected weighted subgraph of the grid $\mathbb{Z}^2$ such that all finite faces are unit squares. Color the vertices of $G$ black. Divide each edge of $G$ in two by inserting green vertices at their midpoints; weight both newly formed edges by the weight of the original edge. Divide each face of $G$ in four by inserting a red vertex at its center and joining it to the green vertices on its boundary by edges of weight 1. Let $\tilde{G}$ be the graph on the black, green and red vertices obtained in this fashion.

THEOREM 11.1 (TEMPERLEY). *If $v$ is a black vertex on the boundary of $\tilde{G}$, then there is a weight-preserving bijection between the spanning trees of $G$ and the perfect matchings of $\tilde{G} \setminus \{v\}$.*

*Proof.* Regard $G$ as being the graph on the black vertices of $\tilde{G}$; let $T$ be a spanning tree of $G$ (see Figures 11.1 and 11.2). For any black vertex $x \neq v$, let $x'$ be the first green vertex encountered along the unique path joining $x$ to $v$ in $T$.
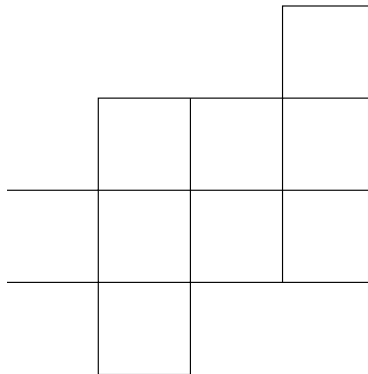


FIGURE 11.1

Next, note that if we include an extra red vertex $u$ for the infinite face of $G$, the red vertices are the vertices of a spanning tree $T^*$ (dual to $T$) of the dual graph of $G$. For any red vertex $y \neq u$, let $y'$ be the first green vertex encountered along the unique path joining $y$ to $u$ in $T^*$.

The collection $\mu_T$ consisting of the edges $\{x, x'\}$, $\{y, y'\}$ with $x$ (resp., $y$) running over black vertices different from $v$ (resp., red vertices different from $u$) is clearly a perfect matching of $\tilde{G} \setminus \{v\}$. Furthermore, the weight of $\mu_T$ is equal to the weight of $T$.

Conversely, let $\mu$ be a perfect matching of $\tilde{G} \setminus \{v\}$. Let $T_\mu$ be the subgraph of $G$ formed by the edges containing some member of $\mu$. Since the members of $\mu$ contained in edges of $G$ are precisely those incident to black vertices, $T_\mu$ has $V(G) - 1$ edges.
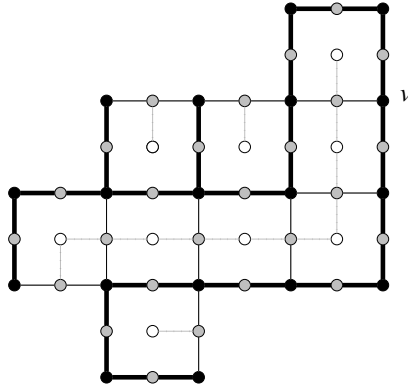
54

FIGURE 11.2

To show that $T_\mu$ is a spanning tree of $G$ it is therefore enough to prove that $T_\mu$ contains no cycle. Suppose this is not the case and let $C$ be a cycle without self-intersections. By induction on the length of $C$ we see that the number of vertices of $\tilde{G}$ encircled by $C$ is odd. Since the removed vertex $v$ belongs to the boundary of the infinite face, it follows that $C$ encircles an odd number of vertices of $\tilde{G} \setminus \{v\}$. However, these cannot be matched by $\mu$, a contradiction. Therefore, $T_\mu$ is a spanning tree of $G$, and its weight is clearly equal to the weight of $\mu$.

Since the maps $T \mapsto \mu_T$ and $\mu \mapsto T_\mu$ are readily checked to be inverse to one another, we obtain the statement of the lemma. $\square$

One nice application of Temperley's trick is a solution to the dimer model on odd square grids with a vertex removed from the boundary. We present this below. Another application will be shown in the next lecture.



FIGURE 11.3

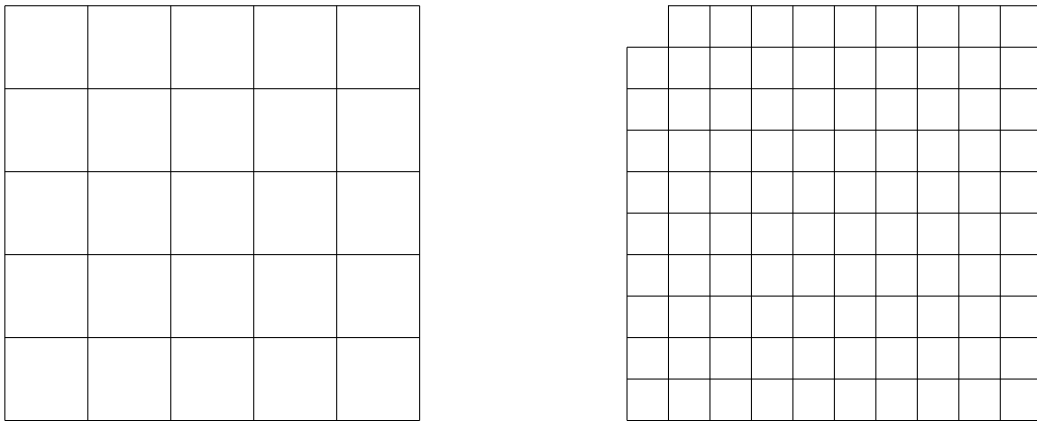Let $G_n$ be the $n \times n$ grid graph ($G_6$ is pictured on the left in Figure 11.3). Denoting by $\mathrm{t}(G)$ the number of spanning trees of $G$, we have by Theorem 11.1 that

$$\mathrm{M}(G_{2n-1} \setminus v) = \mathrm{t}(G_n), \tag{11.1}$$

55

where $v$ is any vertex on the boundary of $G_{2n-1}$ having the same color as the corners in the chessboard-style coloring of its vertices.

We will also employ the following classical result, called the Matrix Tree Theorem.

THEOREM 11.2 (KIRCHHOFF). *Let $G$ be a finite graph, and let $A$ be its adjacency matrix. Let $D$ be the diagonal matrix whose entries record the degrees of the vertices of $G$. Set $M := D - A$. Then if $M'$ is obtained from $M$ by deleting the row and column corresponding to an arbitrary vertex of $G$, we have*

$$\text{t}(G) = \det(M'). \tag{11.2}$$

By (11.1), in order to find $\text{M}(G_{2n-1} \setminus v)$ it is enough to determine $\text{t}(G_n)$. This in turn equals the number of spanning trees of the planar dual $G_n^*$ of the grid graph $G_n$ (we have already used this fact in the proof of Theorem 11.1). Apply Theorem 11.2 to $G_n^*$, choosing to delete the row and column indexed by the vertex $v^*$ corresponding to the infinite face of $G_n$. It is readily seen that the resulting matrix $M'$ is $4I_{n-1} - A_{n-1}$, where $I_{n-1}$ is the identity matrix of order $n-1$ and $A_{n-1}$ is the adjacency matrix of the grid graph $G_{n-1}$. We thus obtain

$$\text{t}(G_n) = \det(4I_{n-1} - A_{n-1}). \tag{11.3}$$

The evaluation of the determinant on the right hand side of (11.3) follows immediately once the eigenvalues of $A_n$ (also called the eigenvalues of $G_n$) are determined. To do this, note that $G_n = P_n \oplus P_n$, where $P_n$ is the path on $n$ vertices and $\oplus$ denotes the cartesian product of graphs (by definition, $G_1 \oplus G_2$ is the graph on $V(G_1) \times V(G_2)$ which has an edge between $(v_1, v_2)$ and $(v_1', v_2')$ iff $v_1 = v_1'$ and $v_2$ and $v_2'$ are adjacent in $G_2$, or $v_2 = v_2'$ and $v_1$ and $v_1'$ are adjacent in $G_1$).

LEMMA 11.3. *Let $\lambda_1, \ldots, \lambda_n$ be the eigenvalues of the graph $G_1$, and $\mu_1, \ldots, \mu_m$ the eigenvalues of the graph $G_2$. Then the eigenvalues of $G_1 \oplus G_2$ are $\lambda_i + \mu_j$, $i = 1, \ldots, n$, $j = 1, \ldots, m$.*

*Proof.* It is readily seen that the adjacency matrix of $G := G_1 \oplus G_2$ is obtained from the adjacency matrix of $G_1$ by replacing the 1's by $I$, the order $|V(G_2)|$ identity matrix, and putting the adjacency matrix $A_{G_2}$ of $G_2$ on the diagonal. Thus $\lambda I - A_G$ is obtained from $\lambda I - A_{G_1}$ by substituting $-I$ for the $-1$'s, and $\lambda I - A_{G_2}$ for the $\lambda$'s.

Since $\lambda I - A_{G_2}$ and $I$ commute, one sees that the matrix achieving the diagonalization of $A_{G_1}$ to $\text{diag}(\lambda_1, \ldots, \lambda_n)$ generates a block-diagonalization of $\lambda I - G$ to $\text{diag}(\lambda I - A_{G_2} - \lambda_1 I, \ldots, \lambda I - A_{G_2} - \lambda_n I)$. This implies that

$$p_G(\lambda) = \det(\lambda I - A_G) = \det \prod_{i=1}^{n} (\lambda I - A_{G_2} - \lambda_i I)$$

$$= \prod_{i=1}^{n} \det((\lambda - \lambda_i)I - A_{G_2}) = \prod_{i=1}^{n} p_{G_2}(\lambda - \lambda_i) = \prod_{i=1}^{n} \prod_{j=1}^{m} (\lambda - \lambda_i - \mu_j),$$

the last equality being due to the fact that the eigenvalues of $G_2$ are $\mu_1, \ldots, \mu_m$. □

Recall that the eigenvalues of the path $P_n$ on $n$ vertices are $2\cos\frac{k\pi}{n+1}$, $k = 1,\ldots,n$. Lemma 11.3 implies then that the eigenvalues of the $(n-1)\times(n-1)$ square grid are $2\cos\frac{k\pi}{n} + 2\cos\frac{l\pi}{n}$, $k,l = 1,\ldots,n-1$. Therefore we have

$$\det(4I_{n-1} - A_{n-1}) = \prod_{k=1}^{n-1}\prod_{l=1}^{n-1}\left(4 - 2\cos\frac{k\pi}{n} - 2\cos\frac{l\pi}{n}\right). \tag{11.5}$$

By (11.1), (11.3) and (11.3) we obtain the following result.

THEOREM 11.4. *If $v$ is any vertex on the infinite face of the $(2n-1)\times(2n-1)$ square grid graph $G_{2n-1}$ having the same color as the corners under the chessboard coloring of the vertices, then*

$$\mathrm{M}(G_{2n-1} \setminus v) = \prod_{k=1}^{n-1}\prod_{l=1}^{n-1}\left(4 - 2\cos\frac{k\pi}{n} - 2\cos\frac{l\pi}{n}\right).$$

# Lecture 12

## Spanning trees of even and odd Aztec rectangles and Aztec rectangles with holes

Suppose the corners of a $(2m+1) \times (2n+1)$ chessboard are black. The graph whose vertices are the unit squares of the board, and whose edges connect *diagonally* adjacent unit squares, has two connected components. The one whose vertices correspond to the white squares is denoted $AD_{m,n}$ and is called the *even Aztec rectangle* of order $(m,n)$; the other is called the *odd Aztec rectangle* of order $(m,n)$, and is denoted $OD_{m,n}$ (for $m=5$ and $n=3$ these are illustrated in Figure 12.1). For $m=n$ the even Aztec rectangle becomes the Aztec diamond graph we have seen several times in this course.
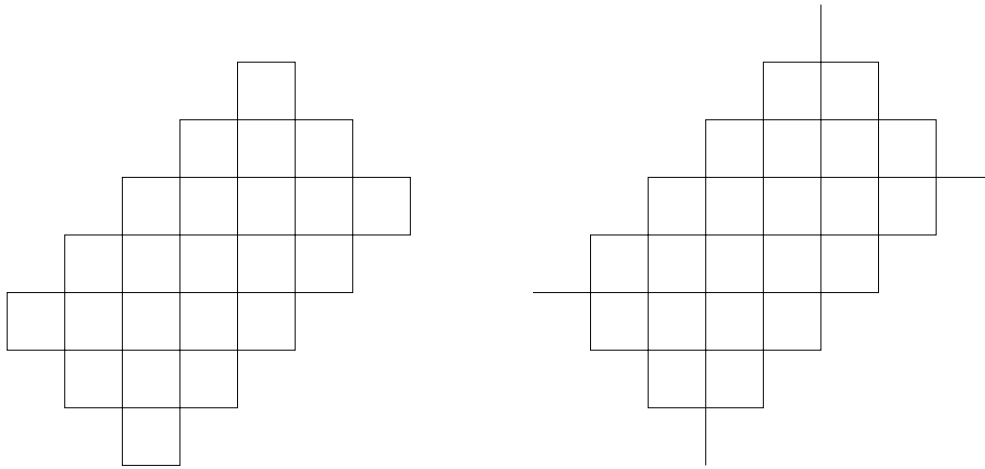


FIGURE 12.1. (a) The even Aztec rectangle $AD_{5,3}$. (b) The odd Aztec rectangle $OD_{5,3}$.

Stanley conjectured that

$$\mathrm{t}(AD_{n,n}) = 4\,\mathrm{t}(OD_{n,n}) \tag{12.1}$$

for all $n \geq 1$, where $\mathrm{t}(G)$ denotes the number of spanning trees of the graph $G$. This was first proved by Knuth by an algebraic method (finding explicitly the spectrum of the graphs). We present here a short combinatorial proof of (12.1) in the case of odd $n$, as a direct consequence of the factorization theorem (Theorem 10.2) and Temperley's trick (Theorem 11.1).

THEOREM 12.1. *For all odd integers $m, n \geq 1$ we have $\mathrm{t}(AD_{m,n}) = 4\,\mathrm{t}(OD_{m,n})$.*

*Proof.* Let $\mathrm{T}(AD_{m,n})$ be the graph obtained by Temperley's construction from $AD_{m,n}$ by choosing $v$ to be the rightmost vertex of $AD_{m,n}$ on its southwest-northeast going symmetry axis (for $m=5$ and $n=3$ this is shown in Figure 12.2(a)). Applying the factorization theorem (Theorem 10.2) to it we obtain

$$\mathrm{M}(\mathrm{T}(AD_{m,n})) = 2^m\,\mathrm{M}(G_1^+)\,\mathrm{M}(G_1^-), \tag{12.2}$$
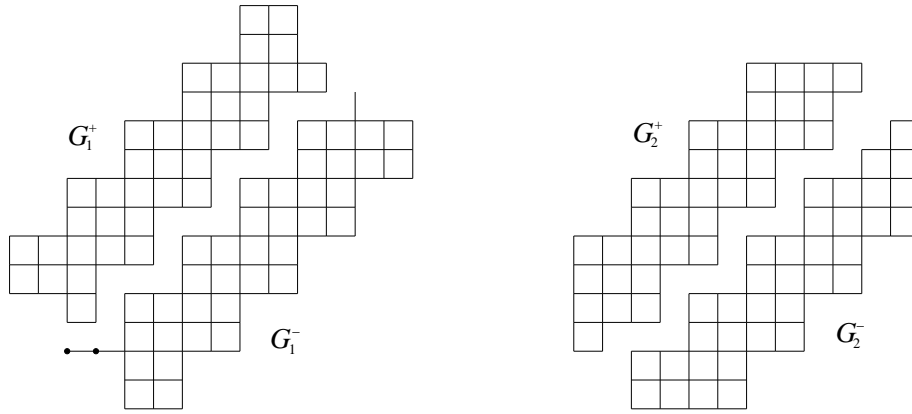
58

Figure 12.3. The effect of the Factorization Theorem on the graphs corresponding by Temperley's construction to: (a) $AD_{5,3}$; (b) $OD_{5,3}$.

where $G_1^+$ and $G_1^-$ are obtained from $\mathrm{T}(AD_{m,n})$ as described in the paragraph before the statement of Theorem 10.2; for $m = 5$, $n = 3$, they are illustrated in Figure 12.3(a).

Before we handle the odd diamond $OD_{m,n}$ similarly, it will be convenient to change slightly its definition, namely by removing its four leaves. This clearly leaves the number of its spanning trees—and thus the statement of Theorem 12.1—unchanged.
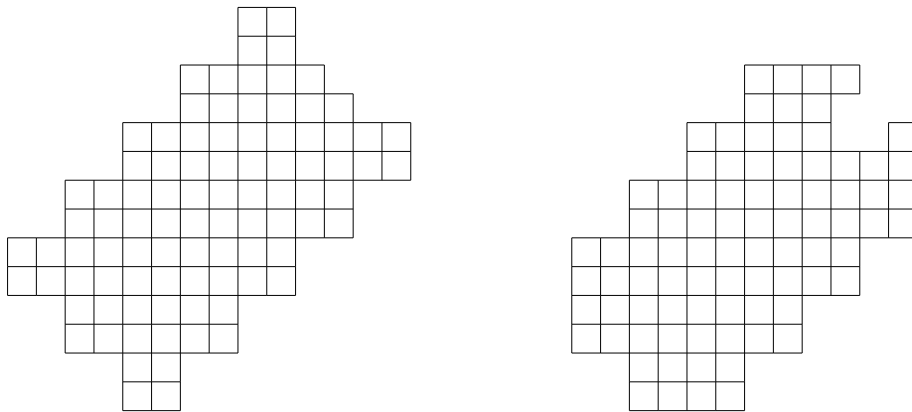


Figure 12.2. Graphs corresponding by Temperley's construction to: (a) $AD_{5,3}$; (b) the graph obtained from $OD_{5,3}$ by removing its four vertices of degree 1.

Let $\mathrm{T}(OD_{m,n})$ be the graph obtained by Temperley's construction from this leafless odd diamond by choosing $v$ to be the rightmost vertex on its southwest-northeast going symmetry axis (for $m = 5$ and $n = 3$ this is pictured in Figure 12.2(b)). Applying the factorization theorem to it we obtain

$$\mathrm{M}(\mathrm{T}(OD_{m,n})) = 2^{m-1}\,\mathrm{M}(G_2^+)\,\mathrm{M}(G_2^-), \tag{12.3}$$

where $G_2^+$ and $G_2^-$ are obtained analogously from $\mathrm{T}(OD_{m,n})$; for $m = 5$, $n = 3$, they are illustrated in Figure 12.3(b).
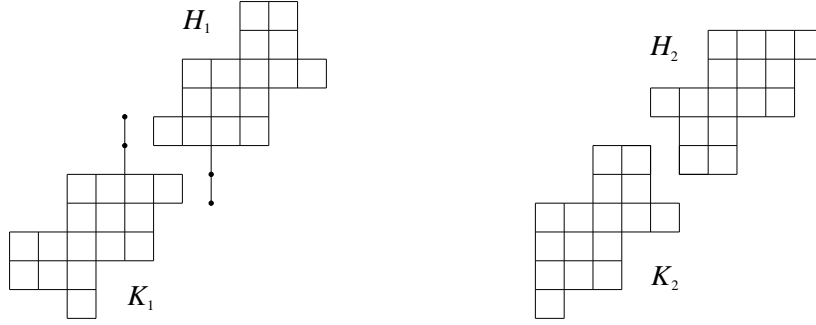
59

Figure 12.4. The effect of the Factorization Theorem on: (a) the top part of Figure 4(a); (b) the top part of Figure 4(a).

Note that $G_1^-$ has two vertices of degree 1, and the edges incident to them must be present in all its perfect matchings. However, the graph obtained from $G_1^-$ by removing the vertices matched by these two forced edges on the one hand, and $G_2^-$ on the other hand, are readily seen to be the results of Temperley's construction applied to isomorphic graphs, with different choices for the removed vertex $v$ (see Figure 12.3). Thus, (12.2) and (12.3) imply

$$\frac{\mathrm{M}(\mathrm{T}(AD_{m,n}))}{\mathrm{M}(\mathrm{T}(OD_{m,n}))} = 2\frac{\mathrm{M}(G_1^+)}{\mathrm{M}(G_2^+)}. \tag{12.4}$$

Furthermore, $G_1^+$ and $G_2^+$ both admit symmetry axes that are diagonal lattice lines (going northwest-southeast). Apply Theorem 10.2 to each of them (for $m = 5$, $n = 3$, this is illustrated in Figure 12.4). We get:

$$\mathrm{M}(G_1^+) = 2^{(n+1)/2}\,\mathrm{M}(H_1)\,\mathrm{M}(K_1) \tag{12.5}$$

$$\mathrm{M}(G_2^+) = 2^{(n-1)/2}\,\mathrm{M}(H_2)\,\mathrm{M}(K_2), \tag{12.6}$$

where $H_1$ (resp., $K_1$) and $H_2$ (resp., $K_2$) are the resulting subgraphs above (resp., below) the symmetry axes in $G_1^+$ and $G_2^+$, respectively. However, one readily sees that the graph obtained from $H_1$ after removing its one forced edge is isomorphic to $H_2$ (being its rotation by $180°$), and the graph obtained from $K_1$ after removing its forced edge is isomorphic to $K_2$ (as it is obtained by reflecting across the horizontal the $90°$ rotation of $K_2$). Thus (12.5) and (12.6) imply $M(G_1^+) = 2M(G_2^+)$, and hence by (12.4) we have $\mathrm{M}(\mathrm{T}(AD_{m,n})) = 4\,\mathrm{M}(\mathrm{T}(OD_{m,n}))$. The statement of the Theorem follows now by Theorem 11.1. $\square$

We conclude by presenting another application of the Factorization Theorem, which generalizes the Aztec diamond theorem (Theorem 2.1).

Let $m$ be even and suppose $m \le n$. Color the vertices of the even Aztec rectangle $AR_{m,n}$ black and white in chessboard fashion, so that all edges have endpoints of different colors. Then the vertices lying on the horizontal symmetry axis $\ell$ are contained in the larger color class. Label them consecutively by 1 through $n$ (see Figure 12.5(a)). For any
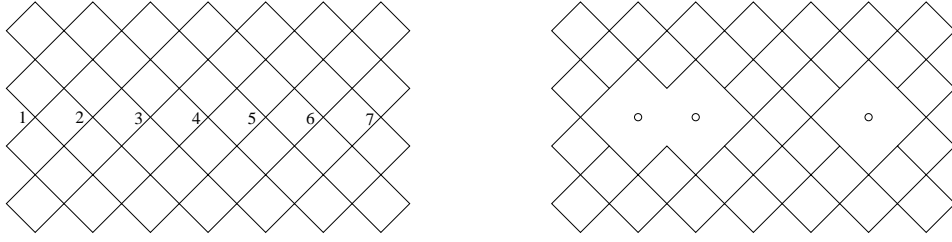
60

FIGURE 12.5(a). The labeling of vertices on $\ell$.   FIGURE 12.5(b). $AR_{4,7}(\{2,3,6\})$.

subset $S$ of $[n] := \{1,\ldots,n\}$ of size $n-m$ define $AR_{m,n}(S)$ to be the graph obtained from $AR_{m,n}$ by deleting the vertices with labels in $S$; an example is shown in Figure 12.5(b).

Note that for odd $m$, the vertices lying on $\ell$ are contained in the smaller bipartition class, and therefore the graphs obtained by the above procedure have no perfect matchings.

THEOREM 12.2. *For $m \le n$ and $m$ even we have*

$$\mathrm{M}(AR_{m,n}(S)) = \frac{2^{m(m+4)/4}}{(0!\,1!\cdots(m/2-1)!)^2} \prod_{1\le i<j\le m/2} (t_{2j-1} - t_{2i-1})(t_{2j} - t_{2i}),$$

*where $[n] \setminus S = \{t_1,\ldots,t_m\}$, $t_1 < \cdots < t_m$.*

Before giving the proof we need some preliminary results. Let $m \le n$ and let $A$ be an $m \times n$ matrix. We say that $A$ is an *alternating sign matrix* if

($i$) all entries are 1, 0 or $-1$
($ii$) every row sum equals 1
($iii$) in reading every row from left to right and every column from top to bottom the nonzero entries alternate in sign, starting with a $+1$.

Let $ASM_{m,n}(S)$ be the set of $m \times n$ alternating sign matrices whose column sums are zero precisely for the column indices belonging to $S$ (note that $|S| = n - m$). We denote by $N_+(A)$ and $N_-(A)$ the number of 1's and $-1$'s in $A$, respectively.

A *monotone triangle* of size $n$ is an $n$-rowed triangular array of non-negative integers such that

($T1$) all rows are strictly increasing
($T2$) the numbers are non-decreasing in the polar directions $+60°$ and $-60°$.

Let us weight every monotone triangle $T$ by $2^{s(T)}$, where $s(T)$ is the number of elements of $T$ that are strictly between their neighbors in the row below, and let $f(t_1,\ldots,t_n)$ be the sum of the weights of all the monotone triangles with bottom row $t_1,\ldots,t_n$. Then a classical result of Mills, Robbins and Rumsey states that

$$f(t_1,\ldots,t_n) = \frac{2^{n(n-1)/2}}{0!\,1!\cdots(n-1)!} \prod_{1\le i<j\le n} (t_j - t_i). \tag{12.7}$$

61

$$
\begin{array}{ccccccc}
0 & 0 & 0 & 1 & 0 & 0 & 0 \\
0 & 1 & 0 & \text{-}1 & 1 & 0 & 0 \\
0 & 0 & 1 & 0 & \text{-}1 & 1 & 0 \\
1 & 0 & \text{-}1 & 1 & 0 & \text{-}1 & 1
\end{array}
\qquad
\begin{array}{cccc}
 & 4 & & \\
 & 2 & 5 & \\
2 & 3 & 6 & \\
1 \quad 2 & 4 & 7 &
\end{array}
$$

$$
\begin{array}{ccccccc}
0 & 0 & 0 & 1 & 0 & 0 & 0 \\
0 & 1 & 0 & 0 & 1 & 0 & 0 \\
0 & 1 & 1 & 0 & 0 & 1 & 0 \\
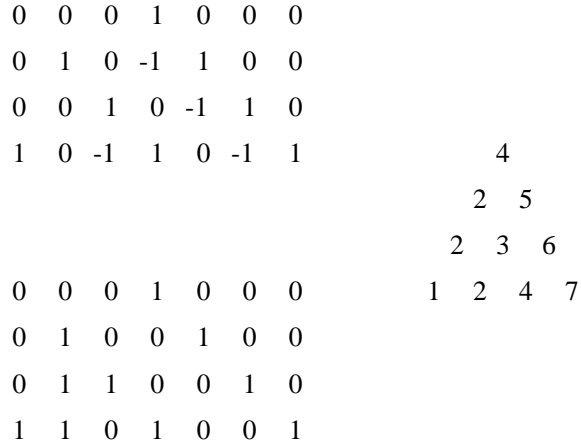1 & 1 & 0 & 1 & 0 & 0 & 1
\end{array}
$$

FIGURE 12.6. A bijection between alternating sign matrices in $ASM_{m,n}(S)$ and monotone triangles with bottom row $[n] \setminus S$.
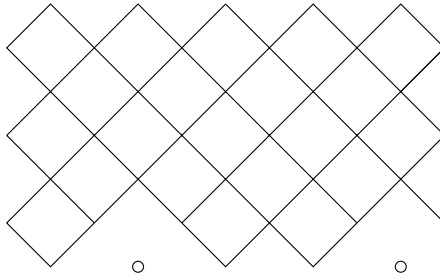


FIGURE 12.7. The graph $\overline{AR}_{3,5}(\{2,5\})$.

*Proof of Theorem 4.1.* Given a matrix $A \in ASM_{m,n}(S)$, let $B$ be the matrix whose $k$th row is the sum of the first $k$ rows of $A$, for $k = 1, \ldots, m$ (see Figure 12.7 for an example). The defining properties of $A$ imply that $B$ is a $0,1$ matrix. Thus, the number of 1's in row $k$ of $B$ clearly equals the $k$th row sum of $B$, which in turn is equal to the sum of the entries in the first $k$ rows of $A$. As all row sums of $A$ equal 1, it follows that row $k$ of $B$ has precisely $k$ 1's. Let $T$ be the triangular array that records the positions of the 1's in the rows of $B$ (see Figure 12.7). Then it is not hard to show that $A \mapsto T$ is a bijection between $ASM_{m,n}(S)$ and the set of monotone triangles with bottom row $[n] \setminus S$, and that $N_-(A) = s(T)$. We obtain therefore

$$
\sum_{A \in ASM_{m,n}(S)} 2^{N_-(A)} = f(t_1, \ldots, t_m). \tag{12.8}
$$

Suppose $k \leq l$ and label the bottom $n$ vertices of $AR_{k,l}$ consecutively from left to right by $1, \ldots, l$. Let $S$ be an $(l-k)$-element subset of $[n]$ and denote by $\overline{AR}_{k,l}(S)$ the graph obtained from $AR_{k,l}$ by deleting the vertices with labels in $S$ (see Figure 12.7 for an example).

Shade the faces of $AR_{k,l}$ in a chessboard fashion so that the edges on the boundary
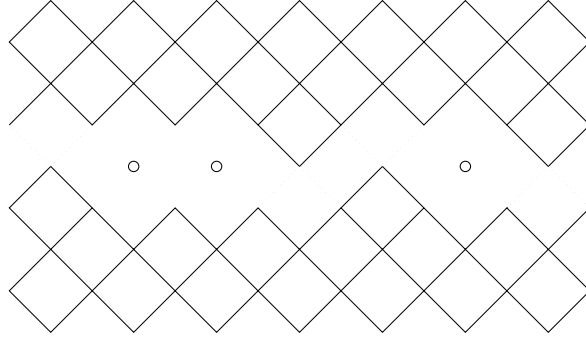
FIGURE 12.8.

belong to shaded faces. By a *cell* we mean a 4-cycle of $AR_{k,l}$ with shaded interior. Let $\mu$ be a matching of $\overline{AR}_{k,l}(S)$. Write in each cell one of the numbers $1, 0$ or $-1$, corresponding to the cases when the cell contains $2, 1$ or $0$ edges of $\mu$. Let $A$ be the $k \times l$ matrix generated in this fashion.

It turns out that the map $\mu \mapsto A$ maps the set of perfect matchings of $\overline{AR}_{k,l}(S)$ to $ASM_{k,l}(S)$, and that each matrix $A \in ASM_{k,l}(S)$ corresponds to precisely $2^{N_+(A)}$ perfect matchings (there are clearly this many choices of $\mu$ on the 1-cells, and it turns out that any of these choices uniquely determine $\mu$; see [**2**] for details). We therefore obtain that

$$M(\overline{AR}_{k,l}(S)) = \sum_{A \in ASM_{k,l}(S)} 2^{N_+(A)}. \tag{12.9}$$

Thus, since $N_+(A) - N_-(A) = k$, we have by relations (12.7)–(12.9) that

$$M(\overline{AR}_{k,l}(S)) = \frac{2^{k(k+1)/2}}{0!\, 1! \cdots (k-1)!} \prod_{1 \le i < j \le k} (t_j - t_i), \tag{12.10}$$

where $[n] \setminus S = \{t_1, \ldots, t_k\}$, $t_1 < \cdots < t_k$.

Apply now the factorization theorem to $AR_{m,n}(S)$, with $\ell$ chosen to be the horizontal symmetry axis. From the definition of the two subgraphs involved in the factorization theorem, it follows that $AR_{m,n}(S)^+$ is isomorphic to $\overline{AR}_{m/2,n}(S \cup \{t_1, t_3, \ldots, t_{2n-1}\})$, and $AR_{m,n}(S)^-$ is isomorphic to $\overline{AR}_{m/2,n}(S \cup \{t_2, t_4, \ldots, t_{2n}\})$ (see Figure 12.8). The result follows then from relation (12.10). $\qquad \square$

**Notes.** The solution of the dimer model on the square lattice (Theorem 1.1) is due independently to Kasteleyn (see [**15**]) and to Temperley and Fisher (see [**23**] and [**11**]; see also [**17**, Problem 4.29]). The enumeration of perfect matchings of honeycomb graphs (Theorem 1.2) is due to MacMahon, who phrased it in the equivalent language of plane partitions (see [**18**]).

The Aztec diamond theorem (Theorem 2.1) is due to Elkies, Kuperberg, Larsen and Propp, who proved it in [**10**]. Lemma 2.3 (the spider lemma) was discovered by Greg Kuperberg. The enumeration of fortress graphs (Theorem 3.2) is due to Bo-Yin Yang ([**25**]). Theorem 3.1 and Theorem 4.1 are presented along with other "perfect powers" enumeration results in [**3**]. Theorem 5.1 is proved in [**2**].

The high temperature expansion is part of the classical statistical physics literature (see for instance [**19**]). The Fisher construction (Proposition 6.2) is due to Fisher, who used it in [**13**] to give a new solution to planar Ising models. Theorem 7.3 was proved by Gallai in [**14**].

The monomer-monomer correlation mentioned in Lecture 8 was introduced by Fisher and Stephenson in [**12**]. Its generalization and the parallels to two dimensional electrostatics are discussed in [**4**], [**6**], [**7**], and [**8**]. The modified Fisher construction (Lemma 8.3) is due to Moessner and Sondhi ([**21**]).

The factorization theorem together with several applications is presented in [**1**]. The connection between spanning trees and perfect matchings stated in Theorem 11.1 is due to Temperley (see [**24**], and for a generalization [**17**, Problem 4.30]). The matrix tree theorem (Theorem 11.2) is attributed to Kirchhoff (see [**17**, Problem 4.9]). Lemma 11.3 is found in [**17**, Problem 11.7]). Theorem 12.1 is presented in [**5**], and Theorem 12.2 in [**1**]. The result expressed in equation (12.7) is due to Mills, Robbins and Rumsey (see [**20**]).

64

# References

[1] M. Ciucu, Enumeration of perfect matchings in graphs with reflective symmetry, *J. Combin. Theory Ser. A*, **77** (1997), 67-97.

[2] M. Ciucu, A complementation theorem for perfect matchings of graphs having a cellular completion, *J. Combin. Theory Ser. A*, **81** (1998), 34–68.

[3] M. Ciucu, Perfect matchings and perfect powers, *J. Algebraic Combin.* **17** (2003), 335–375.

[4] M. Ciucu, A random tiling model for two dimensional electrostatics, *Mem. Amer. Math. Soc.* **178** (2005), no. 839, 1–104.

[5] M. Ciucu,A visual proof of a result of Knuth on spanning trees of Aztec diamonds in the case of odd order, *Discrete Math.* **307** (2007), 1957–1960.

[6] M. Ciucu, Dimer packings with gaps and electrostatics, *Proc. Natl. Acad. Sci. USA* **105** (2008), no. 8, 2766–2772.

[7] M. Ciucu, The scaling limit of the correlation of holes on the triangular lattice with periodic boundary conditions, .*Mem. Amer. Math. Soc.* **199** (2009), no. 935, 1–100.

[8] M. Ciucu, The emergence of the electrostatic field as a Feynman sum in random tilings with holes, *Trans. Amer. Math. Soc.*, in press.

[9] R. Diestel, "Graph theory," Graduate Texts in Mathematics, no. 173, Springer-Verlag, Berlin, 2005.

[10] N. Elkies, G. Kuperberg, M. Larsen, and J. Propp, Alternating-sign matrices and domino tilings (Part I), *J. Algebraic Combin.* **1** (1992), 111–132.

[11] M. E. Fisher, Statistical mechanics of dimers on a plane lattice, *Phys. Rev. (2)* **124**, 1961 1664–1672.

[12] M. E. Fisher and J. Stephenson, Statistical mechanics of dimers on a plane lattice. II. Dimer correlations and monomers, *Phys. Rev. (2)* **132** (1963), 1411–1431.

[13] M.E. Fisher, On the dimer solution of planar Ising models, *J. Math. Phys.* **7** (1966), 1776–1781.

[14] T. Gallai, On factorisation of graphs, *Acta Math. Acad. Sci. Hungar.* **1** (1950), 133–153.

[15] P. W. Kasteleyn, The statistics of dimers on a lattice. I. The number of dimer arrangements on a quadratic lattice, *Physica* **27** (1961), 1209–1225.

[16] D. E. Knuth, Aztec diamonds, checkerboard graphs, and spanning trees, *J. Algebraic Combin.* **6** (1997), 253–257.

[17] L. Lovász, "Combinatorial problems and exercises," North-Holland, New York, 1979.

[18] P. A. MacMahon, "Combinatory Analysis," vols. 1-2, Cambridge, 1916, reprinted by Chelsea, New York, 1960.

[19] B. McCoy and T. T. Wu, "The Two-Dimensional Ising Model," Harvard University Press, 1973.

[20] W. H. Mills, D. P. Robbins, and H. Rumsey, Alternating sign matrices and descending plane partitions, *J. Comb. Theory Ser. A* **34** (1983), 340–359.

[21] R. Moessner and S. L. Sondhi, On Ising and dimer models in two and three dimensions, *Phys. Rev. B* **68**, 054405 (2003).

[22] R. P. Stanley, "Spanning trees of Aztec diamonds," open problem presented at a DIMACS meet ing on Formal Power Series and Algebraic Combinatorics, Piscataway, NJ, May 23–27, 1994.

[23] H. N. V. Temperley and M. E. Fisher, Dimer problem in statistical mechanics—an exact result, *Philos. Mag.* **8** (1961), 1061–1063.

[24] H. N. V. Temperley, "Combinatorics," London Math. Soc. Lecture Notes Series **13** (1974), 202–204.

[25] B-Y. Yang, "Three enumeration problems concerning Aztec diamonds," Ph.D. thesis, Department of Mathematics, Massachusetts Institute of Technology, Cambridge, MA, 1991.